"DEVELOPMENT OF Fe-MoO_3 NANOCOMPOSITE BASED POINT OF CARE DEVICE FOR BREAST CANCER DETECTION"

A DISSERTATION

SUBMITTED IN PARTIAL FULFILLMENT OF THE REQUIREMENTS FOR THE AWARD OF THE DEGREE

OF

MASTER OF TECHNOLOGY

IN

INDUSTRIAL BIOTECHNOLOGY

Submitted By:

AAFRIN SIDDIQUI

2K16/IBT/01

Under the supervision of

Prof. JAI GOPAL SHARMA

DEPARTMENT OF BIOTECHNOLOGY

DELHI TECHNOLOGICAL UNIVERSITY

(Formerly Delhi College of Engineering)

Bawana Road, Delhi-110042

JUNE 2018

DELHI TECHNOLOGICAL UNIVERSITY

(Formerly Delhi College of Engineering)

Bawana Road, Delhi – 110042

CANDIDATE'S DECLARATION

I, Aafrin Siddiqui, Roll no 2K16/IBT/01 of M. Tech (Industrial Biotechnology), hereby declare that the project Dissertation titled " Development of Fe-MoO_3 nanocomposite based point of care device for breast cancer detection" which is submitted by me to the Department of Biotechnology, Delhi Technological University, Delhi in partial fulfillment of the requirement for the award of the degree of Master of Technology, is original and not copied from any source without proper citation. This work has not previously formed the basis for the award of any Degree, Diploma Associateship, Fellowship or other similar title or recognition.

Place: Delhi AAFRIN SIDDIQUI

Date:

DELHI TECHNOLOGICAL UNIVERSITY

(Formerly Delhi College of Engineering)

Bawana Road, Delhi – 110042

CERTIFICATE

I hereby certify that the project dissertation titled "Development of Fe-MoO_3 nanocomposite based point of care device for breast cancer detection" which is submitted by Aafrin Siddiqui, 2K16/IBT/01 (Department of Biotechnology), Delhi Technological University, Delhi in partial fulfillment of the requirements for the award of the degree of Master of Technology, is a record of the project work carried out by the student by my permission and supervision. To the best of my knowledge this work has not been submitted in part or in full for any Degree or Diploma to this University or elsewhere.

Prof. JAI GOPAL SHARMA
(HEAD, DEPARTMENT OF BIOTECHNOLOGY)

Prof. JAI GOPAL SHARMA
(SUPERVISOR)

Place: Delhi

Date:

DEVELOPMENT OF Fe-MoO_3 NANOCOMPOSITE BASED POINT OF CARE DEVICE FOR BREAST CANCER DETECTION

Aafrin Siddiqui

Delhi Technological University,New Delhi.

e-mail: siddiqui.aafreen2013@gmail.com

Abstract

In this work, a new Fe- MoO_3 nanocomposite ITO based electrochemical biosensor is developed, as a robust, sensitive and low-cost point -of-care device for breast cancer detection, using CYFRA21-1 as a biomarker. The Fe-MoO_3 nanocomposite was synthesized by Hydrothermal method, and the Fe content in the nanocomposite was optimized. X-Ray Diffraction (XRD) and scanning electron microscopy (SEM) techniques were used for phase identification and surface morphology analysis of synthesized nanocomposite.(Fe-MoO_3). The 3-aminopropyl triethoxysilane (APTES) was used for the functionalization of Fe-MoO_3, and electrophoretic deposition (EPD) technique was used for deposing it onto ITO coated glass electrode. CYFRA21-1 antibody was immobilized using EDC-NHS, and Bovine serum albumin (BSA) was used to block the non specific active sites. For the immunoelectrode (BSA/anti-CYFRA21-1/APTES/Fe-MoO_3/ITO), electrochemical studies were performed. This biosensor exhibited a linear range of 2ng/ml to 32ng/ml, with the sensitivity of 0.01462mAml/ng, and limit of detection was 0.157 ng/ml. This miniaturized electrochemical setup is simple, portable and is economical.

Keywords: *Breast cancer, biosensor, CYFRA21-1,immunoelectrode, Fe-MoO_3 nanocomposite.*

ACKNOWLEDGEMENT

By the grace of almighty, I express my profound sense of reverence of gratitude to my mentor Prof. Jai Gopal Sharma, Head of the Department of Biotechnology, Delhi Technological University, and my co-supervisor Prof. Bansi. D. Malhotra, Department of Biotechnology, Delhi Technological University, for his valuable guidance, congenial discussion, incessant help, calm, endurance, constructive criticism and constant encouragement throughout this investigation right from the imitation of work to the shaping of manuscript. I am thankful to and fortunate enough to get constant support and guidance to all the faculty members of the Department of Biotechnology.

I am highly indebted to Ms. Shine Augustine (Research Scholar), Ms. Sharda Nara (Post Doctoral, Niharika Gupta (Research Scholar) for their guidance and constant supervision as well as for providing necessary information regarding the instruments and experiments and also for their support in completing the report. At last but never the least, words are small trophies to express my deep sense of gratitude and affection to my labmates and my parents who gave me infinite love to go for this achievement. I am also thankful of Mr. C. B. Singh and Mr. Jitender Kumar for successful submission of my thesis.

AAFRIN SIDDIQUI

(2K16/IBT/01)

CONTENTS

TOPIC

LIST OF TABLE

LIST OF SCHEMES/FIGURES

4.3	FT-IR spectra of (a) MoO_3, (b) Fe-MoO_3, (c) APTES/Fe-MoO_3
4.4	UV Spectra of MoO_3 and Fe-MoO_3
4.5	Dynamic light scattering (DLS) graph of (a) MoO_3 and (b) Fe- MoO_3
4.6	Differential pulse voltammetry (DPV) of MoO_3/ITO, Fe-MoO3/ITO(0.5%), Fe-MoO_3/ITO (2%), Fe-MoO_3/ITO (5%)
4.7	
4.8	Current response of BSA/anti-CYFRA21-1/APTES/Fe-MoO_3/ITO immuno-electrode at different pH values
4.9	Cyclic voltammetry (CV) of anti-CYFRA21-1/APTES/Fe-MoO_3/ITO electrode as a function of scan rate (40-190 mV/s). Magnitude of oxidation and reduction current response as a function of scan rate (mV/s) (inset a), and difference of cathodic and anodic peak potential (ΔEp) as a function of scan rate (inset b).
4.10	
4.11	Electrochemical response of BSA/anti-CYFRA-21-1/APTES/Fe-MoO_3/ITO immuno-electrode as a function of CYFRA-21-1 concentration (2.0-32 ng mL-1).
4.12	Calibration curve between magnitude of peak current and concentration of CYFRA-21-1 (ng mL-1)

LIST OF ABBREVIATIONS

Abbreviations	Full form
Ab	Antibody
APTES	3-Aminopropyl triethoxysilane
SEM	Scanning electron microscopy
BSA	Bovine serum albumin
FTIR	Fourier transform infrared spectroscopy
EDC	N-ethyle-N'-(3-dimethylaminopropyl) carbodiamide
NHS	N-hydroxy succinimide
JCPDS	Joint Committee on Powder Diffraction Standards
PBS	Phosphate buffer saline
XRD	X-Ray diffraction
nMOx	Nanostructured metal oxides
E*pa*	Anodic peak potential
E*pc*	Cathodic peak potential
I*pa*	Anodic peak current
I*pc*	Cathodic peak current
D.I	Deionized water
EPD	Electrophoretic deposition

CHAPTER-1

INTRODUCTION

1) ***Introduction***

Nanomaterials can be defined as the materials whose structural elements lies in the range of 0-100 nm. Their lies a huge classification among nanomaterials i.e they can be clusters, crystals, nanorods, nanobelts nanowires,etc. depending upon the morphology. They have a widespread applications in Drug delivery, Bio-imaging, Nano-medicines, Bio-pharmaceuticals, Biological assays, Cancer therapy etc. *(Salata et al., 2004)*

Biosensor are self analytical devices, which detect and quantify the presence of analytes (samples i.e serum, saliva, blood, sweat, urine etc), using biological elements i.e antibody, DNA, RNA, aptamers, whole cell etc., which when incorporated with appropriate transducing elements, to generate a signal. Basically it is a device which converts the biological signal into electrical signal (*Pandit. S, et al.2016).*

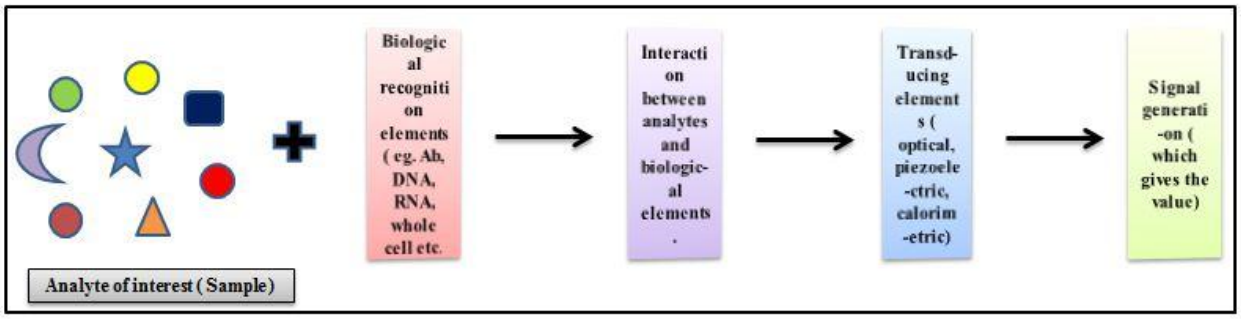

Figure 1.1: Working mechanism of a biosensor

Several types of nanomaterials are widely being used in biosensor fabrication. The use of nanomaterials for the construction of biosensors has improved the sensitivity and performance of them, and has allowed the introduction of many new signal transduction technologies in biosensors. The development of tools and processes used to fabricate, measure and image nanoscale objects, has led to the development of sensors that interact with extremely small molecules that need to be analysed. The two main factor responsible for extensive use of nanomaterials are : Increased surface to volume ratio and Quantum effects.

There are numerous elements, in the periodic table of which nanomaterial's are synthesized eg. Ag, Au, Pt, Zn, Cu etc. among which d block elements prevails in most of the cases. Several physiologically important metals for the human body such as iron, iron oxides, copper, cobalt, and zinc have found an applications in biomedical science. Zinc and zinc oxide nanoparticles are extensively used in sunscreens, biosensors, in cancer therapy, and show no adverse effects. Cobalt nanoparticles have also been used as drug delivery agents and in cancer therapy. *(Sengupta et al.2014).* Apart from all these metallic nanoparticles, molybdenum finds its place

prominently, which is a transition metal with atomic weight 42, belonging to group 6, and period 5, d block element of the periodic table. *(Sengupta et al. 2014).*

Molybdenum oxides are well known materials which are used in chemical research industries (*Oliviria, J.S, et al. 2003).* There exist a wide variety of molybdenum oxides i.e. polycrystalline films, amorphous and crystal films, which can be exploit according to ones need. (*Ramana C.V et al. 2006).* The reasons to choose molybdenum trioxide as a nanomaterial for biosensor fabrication are:

More than one polymorphic form: There are three main polymorphs of MoO3 i.e. orthorhombic α-MoO_3 (thermodynamically stable phase), monoclinic β-MoO3, and hexagonal h-MoO3 (low temperature metastable phase). **Multiple oxidation states**: molybdenum oxides exhibit different oxidation stats of +2, +4 and +6, which in turn facilitates more electron exchange, and increased electrochemical properties for sensing. *(Xu Ruiliang et al. 2013)* **Biocompatibility :** molybdenum trioxide shows the biocompatibility, hence finds its application in bio sensing platform. MoO3 is a high electron affinity oxide because of its closed shell character and the dipole created by internal layer structure. It can have metallic conductivity because of oxygen vacancy is shallow and is easily formed by partial reduction of MoO3.*(Zhao Ye et al.2003).* **Band gap of 3.2 eV:** It is neither too high nor too low, in turn electronic flow from conduction band to valence band can easily occur and a small change in the conductivity can also be measured i.e standard deviation can be detected as well. The other reasons could be crystal structure, chemically stable etc. *(Xu Ruiliang et al. 2013)*

The conductivity of Molybdenum trioxide has been reported to be good, but there is still a scope to increase its conductivity to several folds and for achieving this nanocomposite is one of the best and proven way.

Nano composites are the combination of two different types of materials of which, at least one in nano range, thought to generate not only structural diversity, but also most of the property enhancements. Molybdenum and the various composites of it are widely being used in various sensing field. Molybdenum oxides composites with nickel, lead, iron, copper *(Sundaram R et al.2004).* Molybdenum oxide with graphene oxide, reduced graphene oxide, PANI etc. Sulphide of molybdenum along with the composite are also widely being used in bio sensing platform.

In this work, it is focused to synthesize the nanocomposite of iron and molybdenum trioxide, so that properties of both molybdenum trioxide and iron come into one, with better and improved sensing properties. Reasons for choosing iron in formulation of nanocomposite are:

Iron is one of the biocompatible element. It has been observed that iron can improve the grain size of molybdenum trioxide nanoparticle, when gets incorporated.

Ionic radii of iron is much more smaller than that of molybdenum, which facilitates the ions replacement into the lattice (*Xu, Ruiliang et al. 2013).* The increased sensitivity and electrochemical activity of iron molybdenum trioxide nanocomposite could be explained by the reason below, since the valency of Fe is +2 and +3, and that of molybdenum is +5 and +6, and the ionic radii of Fe is smaller as compare to Mo. So, when Fe enters into the octahedral lattice

of Mo, ion replacement takes place, Fe gets replaced with Mo, due to which lattice distortion takes place, which results into decreased lattice size, due to which size to volume ratio gets increased and exposure to the active sites gets increased, and inturn reactivity is increased *(Ouyang et al., 2012).*

Breast cancer is one of the most common type of cancer, leading to high rate of mortality. There are many types of breast cancer that differ in their capability of spreading to other body tissues. According to the American Cancer society and the National Cancer Institute:

Over 250,000 new cases of invasive breast cancer will be diagnosed each year in women and over 2,400 in men; Approximately 40,610 women and 460 men die yearly;There are over 3.1 million breast cancer survivors in the United States; The five-year survival for all breast cancer patients is nearly 90%.

Causes of Breast Cancer : There are several reasons for the occurance of breast cancer, of which some are genetic and other are environmental factors.
Genetic alterations: Changes occur in some genes (BRCA2, BRCA1, and others) make women more vulnerable to breast cancer. **Family history:** A woman's risk of growing breast cancer is high if her, sister, daughter, mother had it. Studies shows that a women with a family history of breast cancer is more prone of having the disease. *(Kash et. Al, 1994).* **Radiation therapy:** During the childhood Women whose breasts were exposed to radiations are also prone to breast cancer. **Late childbearing:** Women who had their children at a younger age have less chance of developing breast cancer than women who had their first child after the age of 30 or older. *(MacMohan et al., 2006.)*
Conventional detection techniques includes: Biopsy, Fluorescence in situ hybridization (FISH), Immunohistochemistry (IHC).

Drawbacks: Painful sample collection, Time consuming, labor intensive, Highly expensive, require skilled personnel for specimen(collection and analysis).

This has led the researchers a new window and area , where a point of care devices can be developed, for easy, instantaneous, and real time monitoring of breast cancer. There are several types of biomarkers associated , whose levels gets elevated during the diseased condition. According to NCI biomarker is “A biological molecule found in blood, other body fluids, or tissues and is a sign of a normal or abnormal process or of a condition or disease” . A biomarker is "a characteristic that is objectively measured and evaluated as an indicator of normal biological processes, pathogenic processes or pharmacological responses to a therapeutic intervention.” Exists in different forms such as proteins, lipids, carbohydrates and nucleic acids. Some of the biomarker associated with breast cancer are listed below: HER 2 (human epidermal growth factor receptor 2), CEA(carcino embryonic antigen), CGA(chromogranin A), CA(cancer antigen), CYFRA21-1(cytokeratin fragments) *(Mikkelsen, Gastav, et al. 2017).*

CYFRA21-1 is a proteinaceous biomarker is a member of keratin family, that is known to maintain structural integrity of epithelial cells. It is 40kDa in molecular weight and is encoded by

KRT19 gene. (*Rajkumar et al.2015).* it is expressed in higher amount during cancerous condition of oral, breast, and epithelial cancer. It has isoelectric pH of 5.2and is present in intermediate filament of the cytoskeletal structure of normal epithelium and in malignant epithelium, and normal range is 0.5-1.7ng/mL

CYFRA21-1 can be used as a specific biomarker in breast cancer, because of its specificity over other biomarkers. The normal mammary gland is chiefly composed of luminal epithelial cells expressing CK 8, 18, and 19. During breast carcinomas these markers are expressed . (*Brotheri, I, et al. 1998).*

Biomarker	**Sample**	**Normal range (ng/mL)**	**Levels in Breast Cancer (ng/mL**	**Reference**
CYFRA21-1	Serum	0.5-1.7	2.7-3570	Nakata et al. 2000
CYFRA 21-1	Serum	0.2-1.8	3.0 -122	Nakata et al. 2003
CYFRA 21-1	Serum	0.2-1.8	3.0 - 122	Nakata et al. 2004
CYFRA 21-1	Serum	1.93	6.32- 4923	Jung Hyun Yoon et al.2013
CYFRA 21-1	Serum	0.7-3.3	3.9-30	R.Marrakchi et al. 2008
CYFRA21-1	Serum	0.3-1.65	1.65-32	Samia et al. 2016

Table 1.1: Levels of CYFRA21-1 in Breast Cancer

CHAPTER-2
REVIEW AND LITERATURE

Review and Literature

2.1) Nanostructured metal oxide:

Nanostructured metal oxides (NMOs) have recently become important as materials that provide an effective surface for biomolecule immobilization with desired orientation, better conformation and high biological activity resulting in enhanced sensing characteristics. Nanostructured metal oxides with unique optical, electrical and molecular properties along with desired functionalities and surface charge properties provide interesting platforms for interfacing bio recognition elements with transducers for signal amplification The performance of an NMO-based biosensor can be improved by tailoring the properties of the metal oxide–biomolecule interface through engineering of morphology, particle size, effective surface area, functionality, adsorption capability and electron-transfer properties. These interesting NMOs are expected to find applications in a new generation of miniaturized, smart bio sensing devices. The concept of making materials of nanometer size is of fundamental interest. As the size approaches atomic dimensions, energy levels are slowly transferred into quantized discrete energy levels. Further, the reduction in size results in confined electronic motion that affects the physical and chemical properties of materials. Due to the quantum confinement, semiconductor nanoparticles exhibit significant change in their optical and electrical properties. In novel materials, coherent collective oscillations of electrons in the conduction band induce large surface electric field that greatly enhances the radioactive properties when they interact with electromagnetic radiations. This makes the absorption cross-section of these nanomaterial's stronger than the strongest absorption molecules and the scattered light becomes intense than fluorescence of the organic dyes. The concept and ideas to fabricate Nano scale materials derived from chemistry, physics and engineering are integrated to design novel materials with desired properties. Nanomaterial's involve the tailoring of materials at atomic level to attain unique properties, which can be suitably manipulated for the desired application. *(Solanki et al, 2011).*

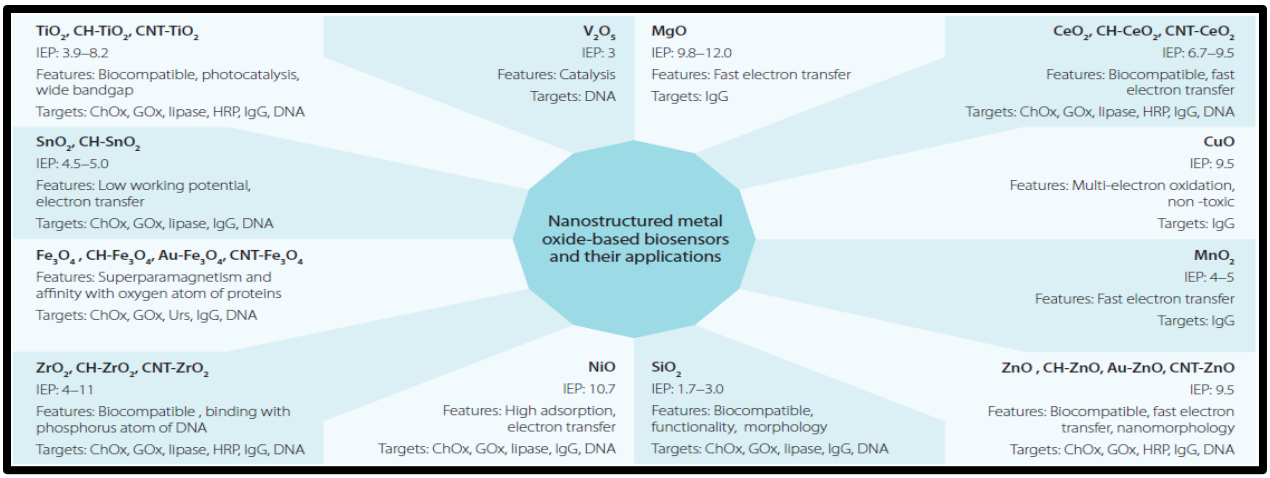

Figure 2.1: Various NMO's used in biosensor fabrication

2.2) Nano composites

Nanocomposites are solid materials that have multiple phase domains and at least one of the phase has a nanoscale structure. Nanocomposite can have a novel chemical and physical properties that depend upon the morphological characteristics of the different materials.

(Nature.com)

2.3) Biosensor:

According to International Union of Pure and Applied Chemistry (IUPAC), biosensor is a self-contained integrated analytical device as it is capable of providing specific semi-quantitative or quantitative analytical information using a biological recognition element. It is used to detect the physio-chemical changes produced by specific interaction between the target analyte and bio recognition element which is detected by a transducer.*(Thevenot et al, 2001*). Bio recognition elements may be antibody, nucleic acid, whole cell or tissue, nucleic acid, receptor protein, enzyme. Biosensor is a self analytical device that detects and quantify the analyte, using biological recognition elements, which when incorporated with appropriate transducer generates a signals. Basically it converts the biological signals into electrical signals In the past decade, biosensors have aroused interest in biomedical and environmental monitoring due to their unique properties like high specificity, portability, speed and low cost.*(Koyun et al, 2012).*

2.4) Components of a biosensor

Biosensor can be classified into five major components:

2.4.1) Analyte or sample:

It is th analyte of our interest means the sample which has to be analysed. It can be blood, serum, saliva, sweat, urine i.e. mainly body secretions. It is taken in a specific quantity for sensing process.

2.4.2) Biological recognition elements:

A biological recognition element such as antibody, DNA, enzyme, aptamer, whole cell, RNA etc. for the recognition of analyte known as bio-receptor. It is the one which is involved in the biological reaction with the analyte of interest., These biomolecular recognition elements should have the ability to recognize biomarkers that are secreted in body fluids such as saliva, urine, sweat, blood etc. Among all these, the most prominent fluid is blood which is commonly used for the detection of biomarkers. The usage of blood sample in biomarkers recognition is invasive, high cost processing and require clinical expert for sample collection, storage, handling etc. that makes the overall process highly complex. To minimize these limitations saliva could be a promising candidate for the detection or analysis of biomarkers.*(Gerard et al, 2002)*

2.4.3) Immobilization matrix:

An immobilization matrix such as nanomaterial's, sol-gel films, self-assembled monolayers and conducting polymers that are used for the immobilization of a biomolecule and An important part of a biosensor is a matrix which is used for the immobilization or integration of desired biological molecules at the surface of transducer. Besides this, matrix should effectively maintain the functionality of the biomolecules and at the same time provides receptivity towards the target analyte and acquainted with the transducer surface. The immobilization method for analyte and operational stability of a biosensor depends upon the chemical properties of immobilizing matrix. The characteristics of a favorable immobilizing matrix it should be resistant to a wide range of physiological temperature, ionic strength, pH and chemical composition.*(Ahuja et al, 2007).*

Among the different types of immobilizing matrices, nanostructured metal oxides achieved a great deal of attention due to their exceptional electronic and optical properties such as high mechanical and thermal stability, larger surface area, biocompatibility, abundant functional groups, and the ability towards the direct electron transfer of proteins or enzymes makes them ideal for the fabrication of a biosensor.*(Ansari et al, 2010)*

2.4.4) Transducer:

A transducer is one which converts biological signal into electrical signal. It is engaged in signal transformation and amplification. Transducer also amplifies the converted signals and produces a recognizable signal. Bio receptor along with transducer is also known as biosensor membrane. Transducer can be classified into different types depending upon the type of signal received such as optical, electrochemical, thermal or piezoelectric transducer. Among them electrochemical transducer aroused much interest due to the simplicity, high signal-to-noise ratio, fast response time and high sensitivity. It offers many advantages over other transducers based biosensor, including lower detection range, high sensitivity, wide linear detection range, good stability, need lower sample amount etc.*(Sinclair,200*)

2.4.5) Electrical and electronic display:

It is the last component of a biosensor, it comprises of all the electronic displays on which the generated signals are displayed, giving the levels of biomarkers in numeric form. It is the one by which the user get to know about the levels.

All these components aggregate together to form a complete working biosensor.

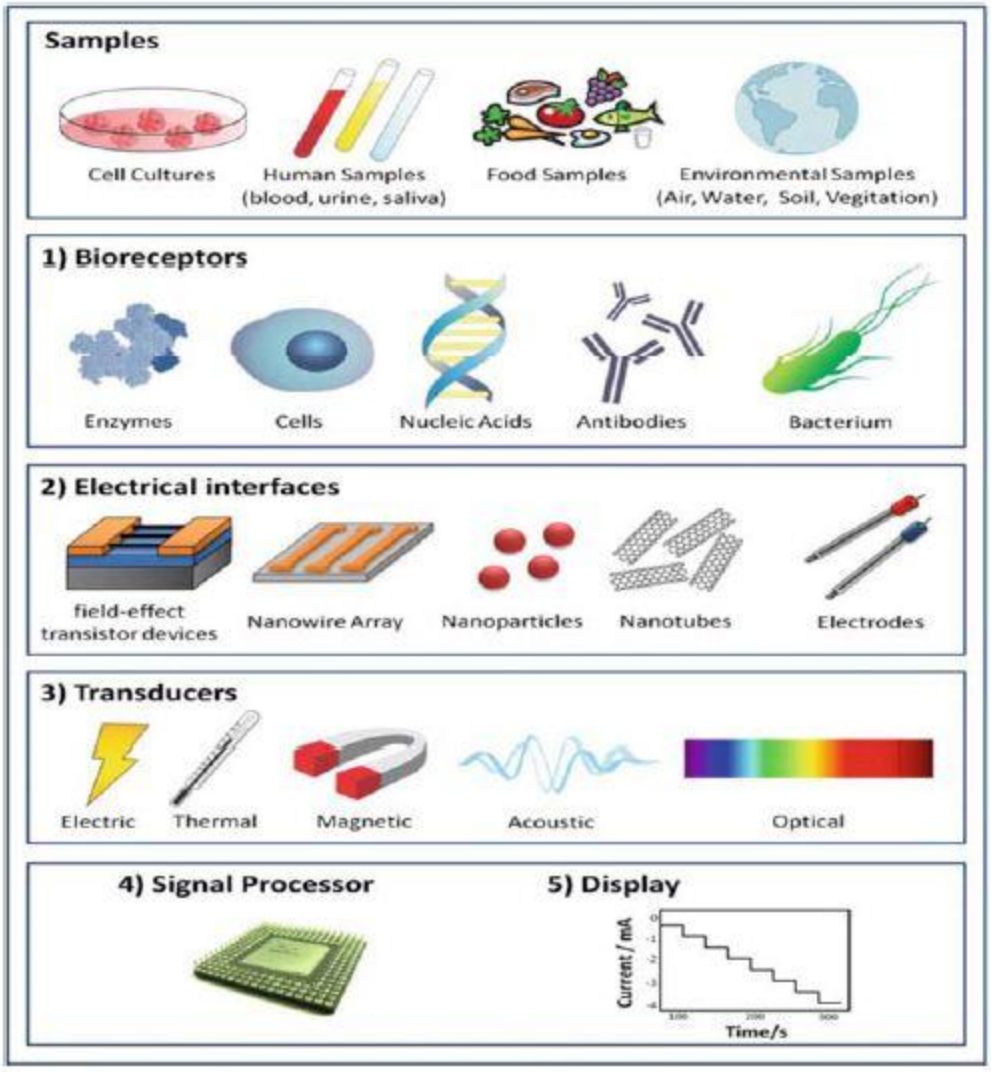

Figure 2.2: Different components of a biosensor *(Ref: Pandit et al, 2016)*

2.5) Cancer:

Cancer is an uncontrolled division of cells with the potential to invade or spread to other parts of the body. Over 100 types of cancer that affects human. Tumors can be classified into two types: begnin and malignant.*(Macaluso et al., 2003)* Not all the tumors are cancerous like begnin tumors do not spread to other parts of the body while malignant tumors spread to other to parts of the body via blood, body fluids etc. The possible symptoms of cancer include lump formation, prolonged cough, abnormal bleeding, loss of weight and change in bowel movements. The factors behind the cause of cancer chewing tobacco, alcohol consumption, poor diet, lack of physical activity, obesity, smoking, exposure to ionizing radiation, hepatitis viruses B and C,

human papilloma virus (HPV) and environmental pollutants. These factors cause changes in genes of a cell that are required before the development of cancer.*(clap et al, 2007).* Sometimes cancer is caused due to inherited genetic defects in person's parents. The use of tobacco causes of about 20% of cancer deaths. In 2012 about 14.1 million new cases of cancer deaths globally. *(Thun et al, 2010).*

2.6) Breast Cancer:

Breast cancer is one of the most common type of cancer, leading to high rate of mortality. There are many types of breast cancer that differ in their capability of spreading to other body tissues. According to the American Cancer society and the National Cancer Institute:

Over 250,000 new cases of invasive breast cancer will be diagnosed each year in women and over 2,400 in men; Approximately 40,610 women and 460 men die yearly; There are over 3.1 million breast cancer survivors in the United States; The five-year survival for all breast cancer patients is nearly 90%.

Causes of Breast Cancer **:** There are several reasons for the occurrence of breast cancer, of which some are genetic and other are environmental factors.
Genetic alterations: Changes occur in some genes (BRCA2, BRCA1, and others) make women more vulnerable to breast cancer.
Family history: A woman's risk of growing breast cancer is high if her, sister, daughter, mother had it. Studies shows that a women with a family history of breast cancer is more prone of having the disease. *(Kash et. Al, 1994).*
Radiation therapy: During the childhood Women whose breasts were exposed to radiations are also prone to breast cancer.
Late childbearing: Women who had their children at a younger age have less chance of developing breast cancer than women who had their first child after the age of 30 or older. *(MacMohan et al., 2006.)*

2.7) Biomarkers in Breast Cancer:

A biomarker is "a characteristic that is objectively measured and evaluated as an indicator of normal biological processes, pathogenic processes or pharmacological responses to a therapeutic intervention." Exists in different forms such as proteins, lipids, carbohydrates and nucleic acids. Some of the biomarker associated with breast cancer are listed below: **HER 2 (human epidermal growth factor receptor 2), CEA(carcino embryonic antigen), CGA(chromogranin A), CA(cancer antigen), CYFRA21-1(cytokeratin fragments)** *(Mikkelsen, Gastav, et al. 2017).*

CYFRA21-1 is a proteinaceous biomarker is a member of keratin family that is known to maintain structural integrity of epithelial cells. It is 40kDa in molecular weight and is encoded by KRT19 gene. (*Rajkumar et al.2015).* it is expressed in higher amount during cancerous condition

of oral, breast, and epithelial cancer. It has isoelectric pH of 5.2and is present in intermediate filament of the cytoskeletal structure of normal epithelium and in malignant epithelium, and normal range is 0.5-1.7ng/mL

Mode of CYFRA21-1 action: In normal cell proteinase is in inactive form, whereas in malignant cells, this proteinase gets activated, and accelerates the cell degeneration. The degeneration of the cell leads to the release of CYFRA21-1, which is soluble in tissues and body fluids. CYFRA21-1 enters into the tissue and body fluids, when release from cell, causes the cell death. (*He, An, et al.2013).*

CYFRA21-1 can be used as a specific biomarker in breast cancer, because of its specificity over other biomarkers. The normal mammary gland is chiefly composed of luminal epithelial cells expressing CK 8, 18, and 19. During breast carcinomas these markers are expressed. (*Brotheri, I, et al. 1998).* CYFRA 21-1 is a fragment of cytokeratin 19, a structure protein and part of intermediate filament proteins necessary for stability of epithelial cells.

Based on data from this prospective single-center study, CYFRA 21-1 could possibly serve as such a biomarker in advanced PC. We could show that pre-treatment CYFRA 21-1 levels are significantly correlated with TTP and OS, and that CYFRA 21-1 may also predict treatment response to chemotherapy. As patients with high CYFRA 21-1 values before the initiation of palliative chemotherapy are less likely to achieve objective disease control, a more intensive treatment (e.g., with the FOLFIRINOX regimen) might be considered in such a poor-prognosis patient population *(Heinemann et al, 2012*). Interestingly, the main determinant for response was the absolute CYFRA 21-1 level (at any of the assessed time points) rather than the kinetics during chemotherapy, an observation that also holds true for CA 19-9 and CEA. When CYFRA 21-1 was analyzed as continuous variable the strongest prognostic information was again based on the absolute CYFRA 21-1 values at each assessed time point and not on the marker kinetics during treatment (*Nakata et al. 2000*).

Material used	**Detection technique**	**Analytes**	**Linear range**	**Limit of detection/ senstivity**	**Normal level of CYFRA 21-1**	**References**
Zirconia on reduced graphene oxide	Electrochemical analysis	saliva	2-22 ng m /L	0.122ng/ mL	0-3.8ng/mL	s.kumar et al 2015
PEDOT:PSS and reduced graphene oxide	Electrochemical analysis	saliva	1-10 ng m/L	25.8µA/ng mL/cm²	0-3.8ng/mL	s.kumar et al 2015
Silanized zirconia nanoparticle	Electrochemical analysis	saliva	2-16 ng m/L	2.2 mA mL ng −1	0-3.8ng/mL	s.kumar et al 2015

	Commercially available kit	Saliva&serum	0.5-50 ng m/ L		0-3.8ng/mL	K rajkumar et al
Hafnium oxide nanoparticle	Electrochemical analysis	saliva	2-18 ng m/L	9.28 µA mL/ng/cm^2	0-3.8ng/Ml	s.kumar et al
Reduced graphene oxide	Electrochemical analysis	saliva	0-30ng/mL	0.16 ng/mL	0-3.8ng/mL	s.kumar et al
Biotinylated alfascreen detection beads	Alpha screen detection kit	serum	0.08-500ng/mL	0.08ng/mL		An he et al 2013

Table2.2: Various biosensors based on CYFRA21-1 biomarker

***2.8) Conventional methods for detection of Breast Cancer* :**

In recent years, number of techniques has been identified to improve the diagnosis and prognosis throughout the body but there is not the similar improvement in diagnosis and prognosis. Because 5 years survival in oral cancer patients is related to the stage at which cancer is diagnose, prevent and early efforts have the chances not only decreases the occurrence, but also improving the survival of those who develop this disease. Many conventional techniques include biopsy, visualization adjuncts, laser capture micro dissection and cytopathology. There are also a number of methods that may contribute to the detection of OC.*(* Some of these are described below:

2.8.1) Biopsy:

In this method, bristled catheter is used to collect the cells sample from the suspected area of OC. It is an invasive technique that is used to diagnose OC. The main drawback of this technique has been associated with brush biopsy is the only means of visualization the OC is poorly identified.

***2.8.2) Cytological techniques*:**

The study of phenotypes and cellular functions of tissues or cells have been done by the different methods of molecular and cell biology. They all come under the cytological techniques.

2.8.3) Laser Capture Microdissection (LCM):

LCM is the technique which boosted the study of cancerous cells on molecular level by providing precise information. It is used to isolated carcinomas from the microscopic regions of tissues or cells with preserved cell morphology. Moreover, with the combination of histochemical staining, we can get more accurate information of cancerous cells. For better molecular diagnostic results, we can use SELDITOF-MS technology with LCM and bioinformatics.

2.8.4) Vital Staining: Toluidine blue has been widely used for staining of cancerous cells. In this method, 1% of aqueous solution of TB has been applied over the lesion for 30 seconds. After that, acidophilic metachromatic nature of TB helps to differentiate between cancerous and normal cells. This staining method has been found to be highly sensitive method to diagnose OC. The major drawback of this technique is about 58% it produce false negative results.

2.8.5) Microscopy: The study of biochemical reaction of cells helps to detection the alteration in cell before the symptoms gets appeared morphologically. Spectral cytopathology (SCP) allow the collection of spectrum from an individual cell and detect internal biochemical changes arise due to disease. SCP works on principles of vibrational spectroscopy for detection of intracellular biochemical changes.

CHAPTER-3

MATERIAL&METHODS

Material and Methods

3.1) Apparatus

Synthesis of Fe-MoO_3 nanocomposite was done by hydrothermal method, using teflon 50 ml stainless steel hydrothermal vessel, purchased from---------. Calcination of the synthesized nanocomposite at 300º C was done using Muffle furnace, MDT- 4310 (Chemtech , India). Ultrasonication of Fe-MoO_3/ACN solution was performed using ultrasonicator, PCI Analytics Pvt. Ltd. Electrophoretic deposition was performed using, electrophoretic equipment GX300C, (Genetix biotech Asia Pvt. Ltd.). Further, image analysis Fe-MoO_3 nanocomposite was done using Scanning electron microscopy (SEM), S-3700N. X-Ray Diffraction (XRD), was performed using, X-Ray Diffractometer (Bruker N8 Advance, U.S.A). UV Spectra of MoO_3 and Fe-MoO_3 solutions were measured using UV-vis-NIR Spectrophotometer, Lambda 950 UV- vis-NIR spectrophotometer. (Perkin Elmer). Electrochemical studies for the synthesized anti-CYFRA21-1/BSA/CYFRA21-1/Fe-MoO_3/ITO immunoelectrode was performed using, electrochemical analyser AUTOLAB- PGT-85279, (Metrohm, India).

3.2) Chemicals and reagents

Sodium Molybadate dihydrate ($Na_2MoO_4.2H_2O$) was procured from Sigma-Aldrich Chemicals.Ferrous sulphate (FeSO4.7H2O), N-hydroxysuccinimide (NHS) [$C_4H_5NO_3$], Potassium ferricyanide {$K_3[Fe(CN)_6]$}, Potassium ferrocnide {$K_4[Fe(CN)_6]3H_2O$}, Sodium Monophosphate [NaH_2PO_4] and Sodium diphosphatedihdrate [$Na_2PO_4.2H_2O$] were purchased from Fischer Scientific. 1-(3-(dimethylamonia)-propyl)-3-ethlcarbodiimide hydrochloride (EDC) [$C_8H_{17}N_3$] analytical grade was purchased from Sigma-Aldrich. (3-Aminopropyl) triethoxy silane (APTES) was procured fron Alfa-Aesar. Concentrated nitric acid was purchased from Rankem Laboratory Reagent. Phosphate buffered saline (PBS) solution of pH 7.0 was prepared using $Na_2HPO_4 \cdot 2H_2O$ (0.05 mol L −1) and NaH_2PO4 (0.05 mol L−1). Fresh PBS solution was prepared using Milli-Q water having resistivity of 18 MΩ cm and stored at 4 °C. All chemicals used were of analytical grade and were not further purified. Biomolecule CYFRA 21-1 antigen

and anti- CYFRA 21-1 were obtained from Raybiotech, which was further diluted to the desired concentration by PBS pH 7.0.

3.3) Instrumentation

a) Hydrothermal Autoclave Reactor:

All the synthesis of nanocomposite were carried out in hydrothermal vessel, purchased from Chemical scientific private limited.. It is a reactor vessel in which hydrothermal synthesis of nanoparticles is carried out, under high temperature and pressure hence it is also called as the hydrothermal bomb, and its operating temperature is 200 ºC. It is made up two chambers that is, one outer chamber made of a good quality stainless steel and second chamber is the inner chamber lined with teflon, which is corrosive resistant. It is also acidic and alkaline resistant, in which the solution of nanoparticle to be synthesized is poured, and sealed with the help of a screw. It has a volume capacity of 50 ml. The autoclave has been designed to use for external heating where the reactor can be heated in the hot air oven, at a specific temperature.

By Hydrothermal synthesis, desired crystalline phases of the nanoparticles can be obtained. It also facilitates the synthesis and growth of directional nanoparticles like Nano rods, due to a very high value of pressure. Also, materials which have a high vapor pressure near their melting points can be grown by the hydrothermal method. The method is also particularly suitable for the growth of large good-quality crystals while maintaining control over their composition.

In this the solutions, with a precursor salts are subjected into the hydrothermal vessel, and put into a hot air oven at 180 ºC, for 42 hrs. After completion of which the nanomaterial is synthesized.

Figure 3.1: Stainless steel Teflon lined Hydrothermal vessel

b) Muffle Furnace

Synthesized nano- composite was annealed using a muffle furnace MDT-4310 (Chemtech, India). Muffle furnace is a type of furnace, which has widespread applications like annealing, sintering, reducing etc. It has a closed chamber of 6*6*12, with a two sided heating element and lined with a cotton wool. The maximum temperature which can be achieved is 950º C. The prepared nanocomposite was put into the furnace at 300 C for 2 hrs, for annealing.

Annealing is a process of heating a material above its recrystallization temperature, maintaining a temperature and then cooling. In Annealing, atoms migrate in the crystal lattice and the number of dislocations decreases, hence internal stress is reduced and better crystal quality is produced, which results in increased crystallinity.

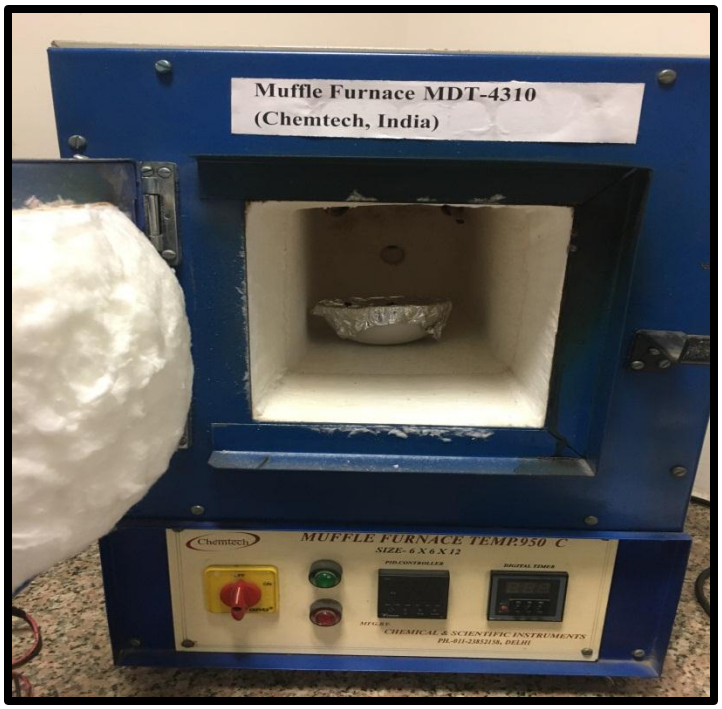

Figure 3.2: Muffle furnace, MDT-4310 (Chemtech, India)

c) Electrophoresis Unit

Electrophoretic deposition (EPD) of synthesized nano composite was performed using electrophoretic unit, GX300C (Genetix Biotech Asia Pvt. Ltd). In EPD there is the movement of nanoparticles under the influence of electric field. Inserting the hydrolysed ITO on working electrode, connected with the negative terminal, and reference electrode connected with positive terminal of the unit. All the parameters and their values are optimised and are set. Fe-MoO3 nanocomposited was deposited onto ITO plate at 50V Potential, current 400mA, and Power 120 W respectively.

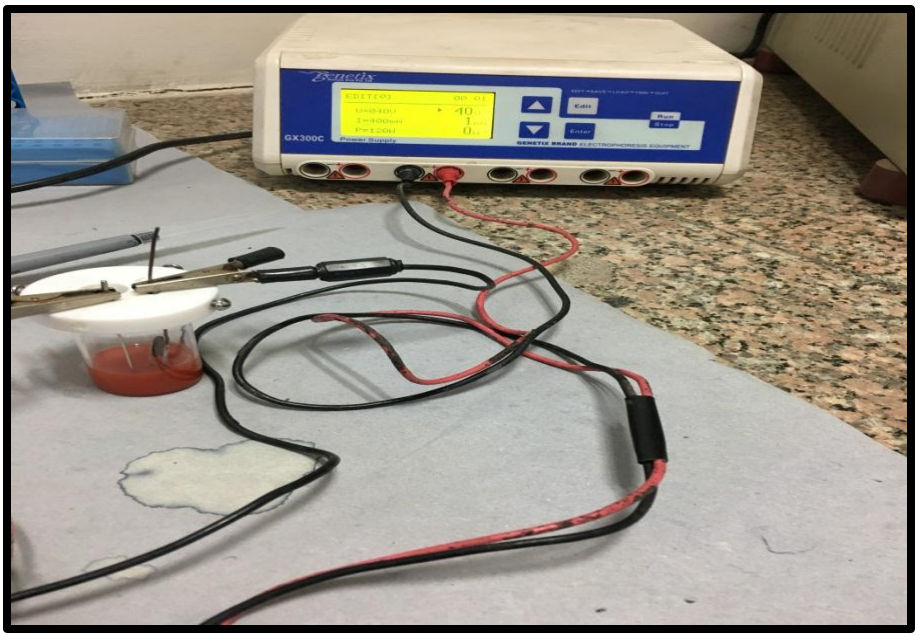

Figure 3.3: Electrophoretic unit GX300C (Genetix Biotech Asia Pvt. Ltd).

d) X-Ray Diffraction (XRD)

XRD studies for the synthesized MoO_3 nanoparticle and Fe-MoO_3 nanocomposite were conducted using Bruker D-8 Advance diffractometer. XRD works on a constructive interference on a monochromatic X-rays on a crystalline sample. The X-rays are generated by a cathode ray tube, filtered to produce monochromatic radiation, collimated to concentrate, and directed toward the sample. The interaction of the incident rays with the sample produces constructive interference (and a diffracted ray) when conditions satisfy Bragg's Law (**Eq. 3.1**)

$$2d \sin\theta = n\lambda \quad \text{..... Eq. 3.1}$$

where λ is the wavelength of electromagnetic radiation, θ is the diffraction angle and d is the lattice spacing in a crystalline sample. These diffracted X-rays are then detected, processed and counted. By scanning the sample through a range of 2θ angles, all possible diffraction directions of the lattice is attained due to the random orientation of the powdered material. This technique is used to characterize the crystallographic structure, crystallite size (grain size) and preferred orientation in polycrystalline or powder solid samples.

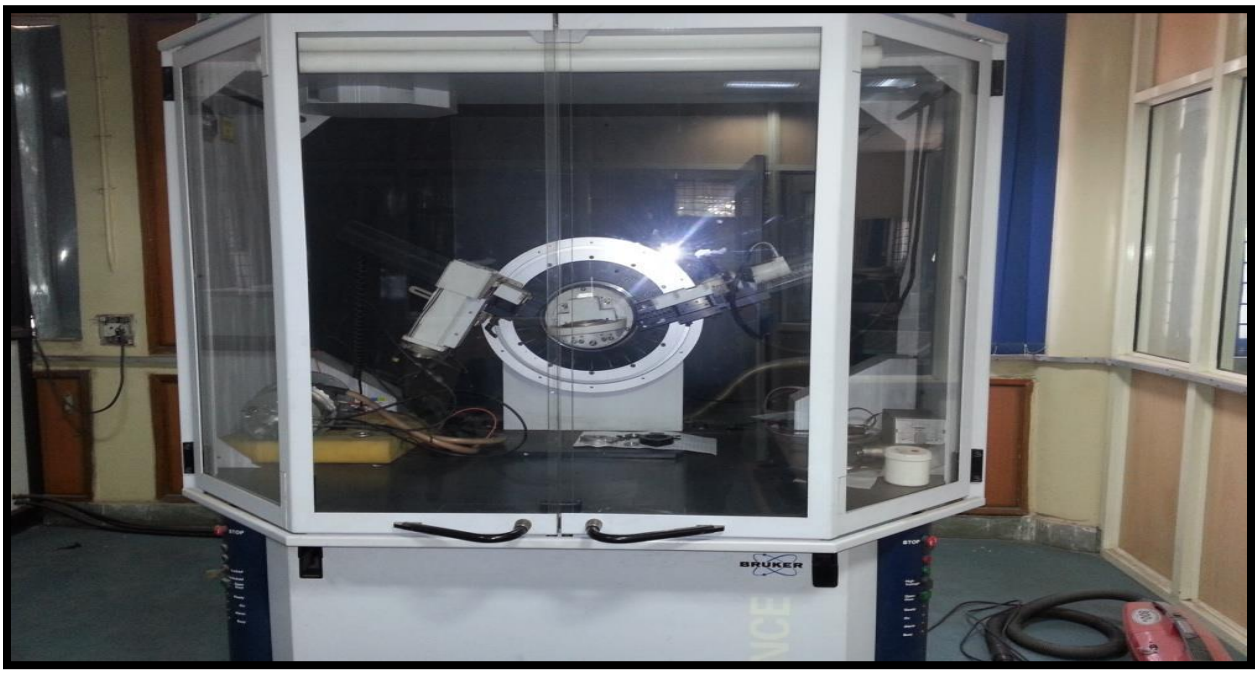

Figure 3.4: X-Ray Diffractometer (Bruker D-8, U.S.A)

XRD can be applied to characterize the heterogeneous solid mixture to determine relative abundance of a crystalline compound. It is also useful in providing information on the structure of unknown sample when coupled with lattice refinement technique such as relative refinement. XRD patterns are recorded on X-ray diffractometer, wherein the peak broadening data are obtained by measuring the average of peak broadening in the five strongest diffraction peaks. The mean size of the nanoparticles is determined from the peak broadening in the X-ray diffraction pattern by using **Debye– Scherrer equation (Eq. 2)**.

$$D = 0.9\lambda / \beta Cos\theta \ldots\ldots\ldots\ldots\ldots \text{ Eq. 3.2}$$

where D is the average crystallite size (Å), λ is wavelength of X-rays (Cu Kα: λ = 1.5418 Å), θ is the Bragg diffraction angle, and β is the full width at half maximum (FWHM) (in radians). The sample under study can be of either a thin layer of crystal or in powder form. Since, the power of a diffracted beam is dependent on quantity of corresponding crystalline substance; it is also possible to carry out quantitative determinations using this technique.

Precautions:

i) The film should be considerably thick to eliminate the substrate interference.

e) <u>Scanning electron microscopy (SEM)</u>

SEM studies were conducted to determine the surface morphology of the synthesized nanocomposite. For this Hitachi S-3700N, Scanning electron microscope was used. This technique utilizes a beam of highly energetic electrons, which determines the objects at a very fine scale. These highly energetic electron beams are generated by a high energy sources, e.g., heated tungsten, and scanned over a specimen. As the beam hits the sample, electrons and X-rays are ejected from the sample which is collected by detectors and processed to produce a visual image of the fine structure of the sample. The 10 nm resolution of SEM allows the visualization of materials at sub- micron levels.

<u>Figure 3.5: Scanning electron microscope (Hitachi S-3700N, Japan)</u>

An attachment called Energy dispersive X-ray spectroscopy is also used in SEM for the elemental analysis of the specimen. Here, X-ray spectrometer converts X-ray photon into an electrical pulse which is measured by a multi-channel analyzer. The analyzer records increments in corresponding "energy slot" and shows on a monitor display. The location of the slot is proportional to energy of the X-ray photon entering the detector. The display is a histogram of the X-ray energy received by the detector, with individual peaks, the heights of which are proportional to the amount of a particular element in the specimen being analyzed.

Precautions:

i) If the sample conductance is poor then a few Å thick conductive gold coating should be done by sputtering before analysis in order to have better resolution.

ii) The dimension of the sample should be ~ 0.5 cm × 0.5 cm.

f) Fourier transform infrared (FT-IR) spectroscopy

FT-IR studies for the synthesized nano composite were conducted on Perkin-Elmer instrument. FT-IR is an analytical technique used for the structural characterization of organic materials. It is based on specefic infrared absorption displayed by molecular bonds depending upon their vibrational states. In the FT-IR spectra, the appearance or non- appearance of certain vibrational frequencies gives valuable information about the structure of a particular molecule. Each functional group has a specefic range of vibrational frequencies and is very sensitive to the chemical environment, thus providing information about the presence of functional group in the sample for further characterisation. It has a spectrum range of 400-4000 cm^{-1}.

g) UV-Vis spectrophotometer

UV-VIS spectroscopy were used for detecting the presence of the elements in synthesized MoO3 and Fe-MoO3 nanocomposite. The UV readings were taken from Perkin-Elmer, Lambda 950 UV-vis-NIR Spectrophotometer. It provides the detailed information about the optical properties of samples including the nanomaterial's. Since the electronic transitions require the radiation from the UV and visible region of the electromagnetic radiation spectrum, it is often called UV-visible or UV-vis spectroscopy. This technique provides a convenient platform for detection of analytes and their concentration in a solution.

It is based on Beer-Lambert Law which states that the fraction of incident radiation absorbed is proportional to the number of absorbing molecules in its path. The amount of light absorbed or transmitted by a solution, directly depends on the concentration of the solute and length of the path travelled by radiation through the sample.

The peak intensity of absorption spectrum is directly proportional to the number of molecules absorbing light of a specific wavelength.

Hence,

$$\textbf{Log Io / I} = \varepsilon \, c \, l$$

where,

c: concentration of the solute in mol l-1, l: path length of the sample in cm, whereas Io and I are the intensity of the incident light and intensity of light transmitted through the sample solution, respectively. ε represents the molar extinction coefficient dependent on absorbing species in a particular solvent at a particular wavelength. The ratio I / Io is known as transmittance T while the logarithm of the inverse ratio Io / I indicates the absorbance A.

.h) Electrochemical analyser:

All the electrochemical studies reported were performed using an Autolab Potentiostat/Galvanostat (AUT-85279, Metrohm, India). The studies were conducted using three electrode system, with anti CYFRA21-1/BSA/APTES/Fe-MoO_3/ITO immunoelectrode on working electrode made up of copper, Ag-AgCl and platinum as reference and counter electrodes. PBS solution (0.1 M; pH 7) as redox species used as an electrolyte.

Figure 3.6: AUTOLAB, potentiostat/galvanostat (AUT-85279, Metrohm, Switzerland).

Electrochemical techniques relate the changes of an electrical signal to an electrochemical reaction at an electrode surface, usually as a result of an imposed potential or current. In a solution, the equilibrium concentrations of the reduced and oxidized forms of a redox couple are linked to the potential (E) via the Nernst's Equation (Eq. 4.3).

$$E = E_o + \frac{RT}{nF} \ln \frac{Coxi}{Cred} \quad \text{..... Eq. 3.3}$$

where, *Eo* is equilibrium potential, *F* is Faraday's constant, *T* is absolute temperature, *Coxi* and *Cred* are concentrations of oxidation and reduction centers.

Differential pulse voltametry:

DPV is one of the most widely used pulse techniques in electrochemistry. Electrochemical pulse methods involve the modulation of potential in order to increase speed and sensitivity of measurement. DPV consists of a series of potential pulses of fixed amplitude (10-100 mV) superimposed on to a slowly changing base potential. The time interval of each potential step in this series is ~40-50 ms. The current is measured at two time points of the pulse – first, just before the pulse starts and second when the pulse ends. The difference between the current

values at these two points (δi) is plotted against the base potential. The resulting plot of δi vs. V is referred to as a differential pulse voltammogram consisting of current peak(s), the height of which is directly proportional to the concentration of the corresponding analyte. The relationship between the peak current and concentration of analyte is given by the expression –

$$\mathbf{Ip} = \boldsymbol{nFAD}\mathbf{1/2}\boldsymbol{C}\ \sqrt{(\mathbf{1}-\boldsymbol{\sigma})(\mathbf{1}+\ \boldsymbol{\sigma})}\ \ldots\ldots\ldots\ldots\ \mathbf{(3.4)}$$

where n is the no. of electrons involved, F is Faraday's constant, A is electroactive surface area, D is diffusion coefficient, C is the concentration of the electroactive species, tm is the time after pulse when current is sampled, and σ = exp[(nF/RT)(ΔE/2)] (ΔE is the pulse amplitude). For large values of ΔE, the maximum value of (1-σ)/(1+σ) is unity.

The value of charging current is mathematically described by the following equation –

$$\boldsymbol{Ic} \approx -\mathbf{0.00567}\boldsymbol{CCi}\Delta\boldsymbol{Em}\mathbf{2/3}\boldsymbol{t}-\mathbf{1/3}\ldots\ldots\ldots\ldots\ldots\ \mathbf{(3.5)}$$

where Ci is the integral capacitance. It is clear from the above equation that the 'differential-pulse' operation leads to a fast decay of charging current. This decreases the contribution of charging current to the faradaic current leading to accurate results. In other words, DPV offers an added advantage of lower charging current and allows measurements at concentrations as low as 10-8 M (Wang, J, 2006). Any unknown analyte involved in the redox reaction can be determined by the peak potential (Ep) as it is related to the half-wave potential by the following equation –

$$\mathbf{Ep = E1/2 - \Delta E/2}\ \ldots\ldots\ldots\ldots\ \mathbf{(3.6)}$$

The peak width at half-height can be used to determine the number of electrons involved in the reaction by the following equation –

$$\boldsymbol{W}\mathbf{1/2}=\mathbf{3.52}\boldsymbol{RTnF}\ \ldots\ldots\ldots\ldots\ \mathbf{(3.7)}$$

Thus, a one-electron stoichiometry corresponds to a peak width of 30.1 mV at room temperature *(Wang et al, 2006).*

<u>Cyclic voltammetry</u>

Cyclic voltammetry is the study of current variation over a range of electrode potentials, at which the electrodes are operated. The same potential window is then scanned in the reverse direction,

means starting from the negative value to the positive value of the applied voltage, hence termed as cyclic. A graph is plotted between current and voltage, which is known as cyclic voltammogram. The electroactive species produced by oxidation on the forward scan gets reduced on the reverse scan if the process is reversible in nature. CV is used to study the electrochemical properties of substances in both solution state and also at the electrode interface. Cyclic voltammogram is sigmoid shape graph, obtained both at positive and negative x –y axis, which gives the values of cathodic and anodic peak potential (Epc, Epa) and cathodic and anodic peak current (Ipc, Ipa). CV also determines the electrode potentials required for the oxidation or reduction of different redox species (i.e mediators). During oxidation and reduction, the mediator shows a peak on the cyclic voltammogram, depending upon the redox reaction is reversible.

3.4) Experimental

3.4.1) Hydrothermal method

It is one of the method through which nanoparticles are synthesis, at a very high temperature and pressure.. It is carried out in a specialized type of vessel known as autoclave. The time and the temperatures are set according to the type of nanomaterial which has to be synthesized. Generally the temperature for the synthesis is 180 ºC. Depending upon the nature of nanomaterial time also varies from 24 -42 hrs. Hydrothermal method is performed in order to get the crystal structure, and crystal growth takes place in the autoclave itself. This method is preferred, generally for the synthesis of directional nanomaterial's i.e. nanorods, etc.

Advantages of the hydrothermal method over other types of crystal growth include the ability to create crystalline phases which are not stable at the melting point. Also, materials which have a high vapour pressure near their melting points can be grown by the hydrothermal method. The method is also particularly suitable for the growth of large good-quality crystals while maintaining control over their composition. Disadvantages of the method include the need of expensive autoclaves, and the impossibility of observing the crystal as it grows and also aggregation of nanoparticles also occurs

3.4.2) Synthesis of Molybdenum trioxide nanoparticles

The molybdenum trioxide nanoparticles were synthesized by Hydrothermal Method.
First of all 600 mg of sodium molybdate dehydrate was added to the 25 ml of Distilled water and was kept for vigorous stirring for 45 mins at 350 rpm. Then 2.5 ml of concentrate HNO_3 was added into the solution and was continuously stirred at 350 rpm at room temperature for 2 hrs, until the Ph of the Mixer solution pH was 1 and colour becomes pale yellow. The mixer solution was then transferred into a 50 ml Teflon vessel and was placed in a stainless steel tank sealed and maintained at temperatures (T = 180 $^{\circ}$C) for 36 hours placed in an hot air oven. The obtained precipitates were separated by centrifugation at 7000-8000 rpm, washed with distilled water and 70 % ethanol and finally dried in hot air oven at 80 $^{\circ}$C for 24 hrs. Mortar pestle was used to crush the dried molybdenum trioxide nanoparticles into powder form, which was further annealed at 300ºC for 2 hrs, in muffle furnace. Finally the synthesized molybdenum trioxide nanoparticles were collected.

600 mg sodium Molybdate dehydrate (precursor salt) was added to the 25 ml of Distilled water and vigorous stirring it at 350 rpm, at room temp. for 45 min, the solution become colourless

.

Add 2.5 ml of concentrate HNO_3 was introduced into the solution and continuously stirred at 350 rpm, at room temperature for 2 h. Mixer solution pH is 1 and colour becomes pale yellow.

.

The solution thus obtained was transferred into a 50 ml Teflon vessel and placed in a stainless steel tank, sealed and maintained at temperatures (T = 180 ◦C) for 36 hours placed in an oven.

The obtained precipitates were separated by centrifugating the solution at 7000-8000 rpm, washed with distilled water and 70% ethanol and finally dried in hot air oven at 80 ˚C for 24 hours

Mortar pestle was used to crush the product into powder form, which was annealed at 300º C for 2 hrs, in muffle furnace.

Reaction involved:

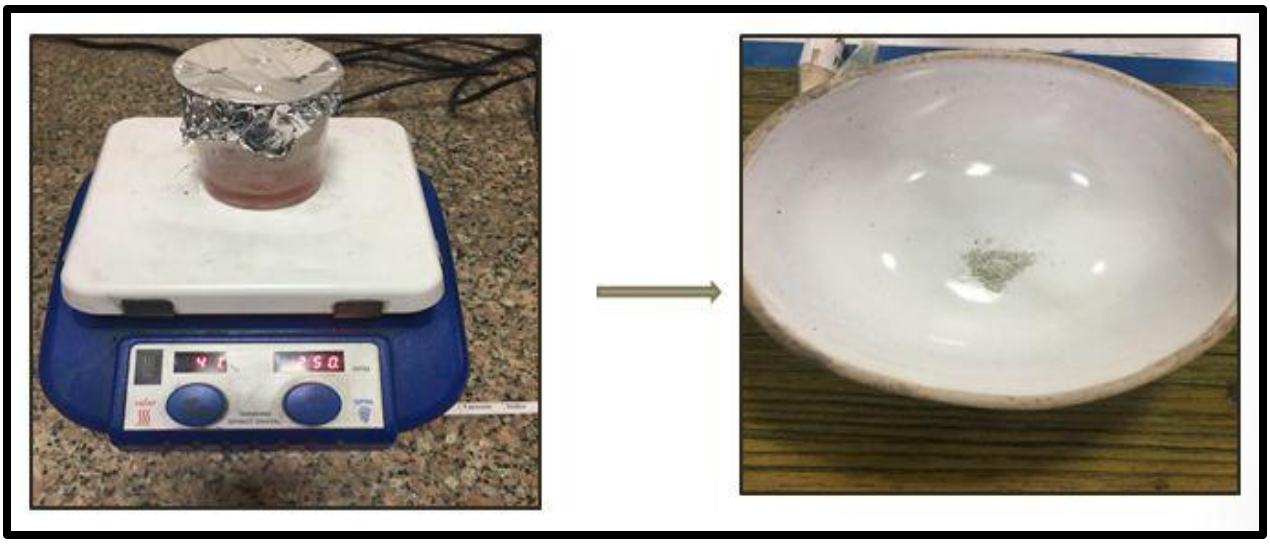

Figure 3.7: Synthesis of MoO_3 nanoparticle via Hydrothermal method

3.4.3) Synthesis of Iron-Molybdenum trioxide nanocomposite

Synthesis of Fe-MoO3 nanocomposite was carried out using the above described Hydrothermal Method. 600 mg of sodium molybdate salt was taken, into which 25 ml D.I water was added and kept on stirring, at 350 rpm for 1 hr. Then to the obtained solution, 300 mg of ferrous sulphate was added, and further stirring at 300 rpm was carried out, for 1 hr, at room temperature. Further 2.5 ml of conc.nitric acid was added into it, and was stirred at 350 rpm for 2 hrs, which was then transferred into to 50 ml Teflon vessel and placed it in stainless steel hydrothermal vessel at 180 º C for 36 hrs. Precipitate were separated by centrifugation technique, at 7000-8000 rpm, and washing was done with 5-6 times D.I and 1-2 times with 70% ethanol, and was dried at 80ºC for 24hrs in oven, finally crushed using mortar and pestle and was annealed at 300º C for 2 hrs in muffle furnace. Finally the synthesized iron molybdenum trioxide nanocomposite was collected for further experimentation.

.

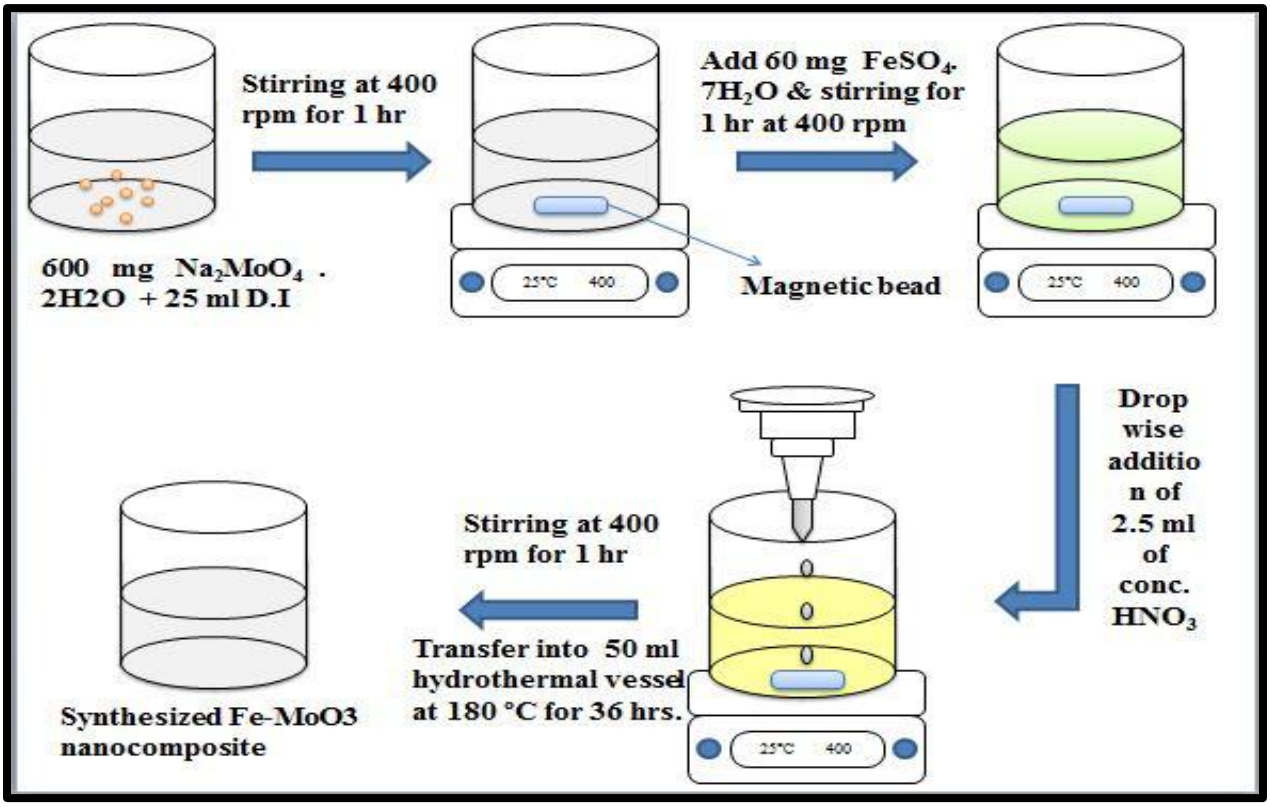

Figure 3.8: Procedural step for the synthesis of Fe-MoO_3 nanocomposite

3.4.4) Functionalization of synthesized Fe-MoO3 nanocomposite

Functionalization of the synthesized Fe-MoO_3 nanocomposite was done using 3-Aminopropyl) tri-ethoxy silane (APTES). *Gunda ,N, et al. 2014)* For which, a dispersed solution consisting of 100 mg of Fe- MoO_3 nanocomposite was added to 20 ml of isopropanol and stirred at 300 rpm, to obtain a highly dispersed suspension. Into which, 200µl of 98% APTES and 10 ml of Distilled water was added, and the solution mixer was mixed and kept on continuous stirring at 300 rpm for 48h at room temperature (25 ^{o}C). In order to remove the unbounded APTES, the

suspension was centrifuged and washed thoroughly with deionized water and ethanol 5-6 times respectively, finally kept in a hot air oven for drying at 60 ^{o}C for 18 h, post of which APTES functionalized Fe-MoO3 nanocomposite were obtained.

3.4.5) Fabrication of bio sensing platform:

Fabrication of bio sensing platform, depict the deposition of synthesized nanocomposite onto the pre-hydrolyzed ITO coated glass electrode, which is followed by the immobilization of antibody i.e. CYFRA 21-1 via drop cast method, which is then used for further sensing.

i. Hydrolysis of ITO electrode

The ITO coated glass electrode having a specific dimension is hydrolyzed via a process called hydrolysis. This is a process which is performed to expose the –OH group onto the ITO glass electrode surface, which in turn facilitates the effective binding of the nanomaterial onto it, in other words it can be said that a thin and uniform film of nanomaterial is formed. First of all, the conductive surface of the ITO glass electrode is checked using multimeter, then a solution of NH_3, H_2O_2, and H_20 in the ratio of 1:1:5 is prepared and ITO slides are dipped into the prepared solution in the glass petri plate, with conductive surface on the upper side. Now this petri plate are kept in hot air oven at 80 º C for 1 hr. After completion of the time it is then removed from the hot air oven, and is washed with D.I water 3-4 times and finally with ethanol.the finally hydrolysed ITO electrode are kept at room temperature till further use.

Figure 3.9: Conductivity measurement of the hydrolyzed ITO electrode

ii) ***Electrophoretic deposition (EPD)***

EPD is the deposition of synthesized nanocomposite onto the ????????? ITO or any conductive substrate . In this work,the pre- hydrolyzed Indium Tin Oxide (ITO) coated glass electrode has been used as conductive substrate. For, the deposition of synthesized Fe-MoO_3 nanocomposite, it is suspended in a liquid medium, under the electric field, and were deposited onto the conducting (ITO) surface. Initially a colloidal solution of Fe-MoO_3 (1mg mL^{-1}) was prepapred by mixing 12 mg of Fe-MoO_3 nanocomposite in 12 ml of Acetonitrile (ACN) solution, followed by sonicvation for 2 hrs,. Colloidal suspension, thus obtained was transferred into a glass cell, for EPD using two electrode system. The ITO electrode was fixed onto the working electrode and the platinum as reference electrode kept at 1 cm . The circuit was completed by fixing the crocodile pins onto the working elctrode (-ve) and reference electrode (+ve). After the optimization of at different voltage and time the final optimized values of for synthesized nanoparticles, and nanocomposite were obtained as, MoO_3 : 50 V, 2 mins. For Fe- MoO_3: 55 V, 2 mins and for APTES/ Fe-MoO_3: 50 V, 1 min.

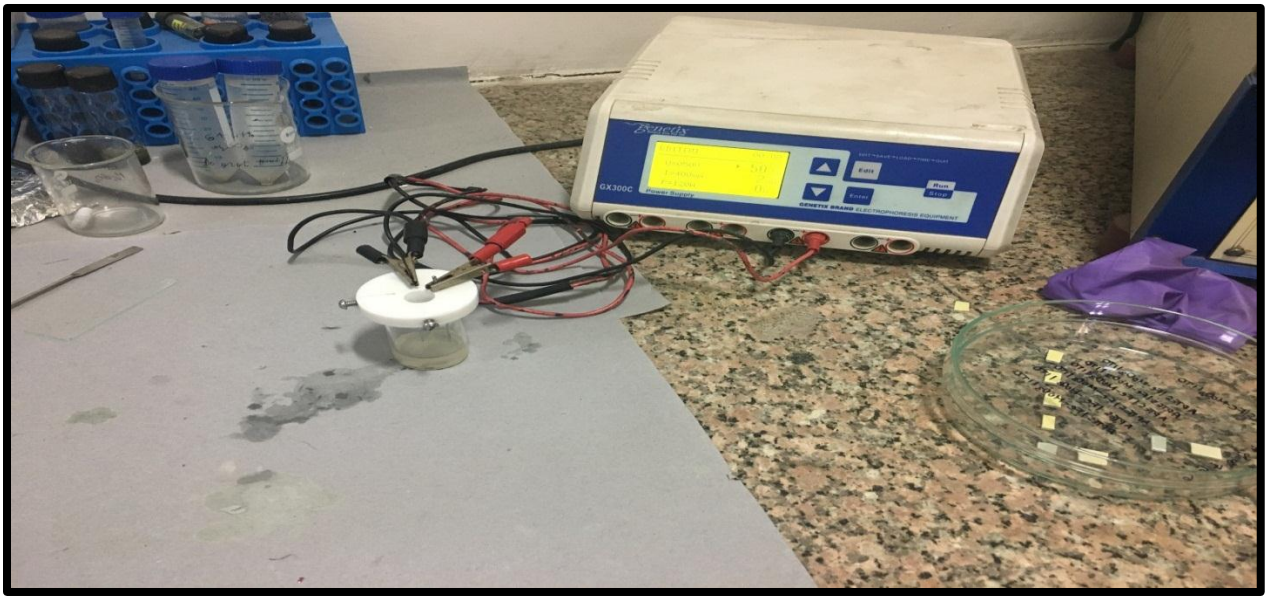

Figure 3.10: Electrophoretic deposition of /APTESFe-MoO_3 nanocomposite onto pre-hydrolyzed ITO electrode

iii) Immobilization of CYFRA21-1 onto the APTES/Fe-MoO3/ITO:

It is a process of attaching the anti-CYFRA21-1 onto the fabricated APTES/Fe-MoO_3/ITO electrodeVia drop cast method.Immobilization o f the antoibody ionto the fabricated platform was carried out via covalent chemistry . here anti-CYFRA21-1 and EDC-NHS were taken in ration 1:1. In brief , 50 µl of 2 ug mL ?????????????? of anti-CYFRA21-1 mixed in 1.5 ml ependroff, with 25µl 0.4 M of EDC and 25µl of 0.1 M NHS, and left for 30 mins, for incubation. Here EDC and NHS acts as a coupling agents. EDC is a carbodiimide that acts as an activator, that activates the –COOH group present on antibody CYFRA21-1, so that it could bind with the $–NH_2$ group present on the APTES/Fe-MoO_3. NHS acts as a stabilizer which stabilizes these two groups for further reaction. The stabilization is done by converting the amine reactive esters intermediate to amine-reactive sulpho NHS ester and also it increases the efficiency of the reaction. After incubation 20µl is poured onto each fabricated APTES/Fe-MoO_3/ITO electrodeThe electrode thus obtained was called as anti-CYFRA21-1/APTES/Fe-MoO_3/ITO electrode, also known as immune electrode. This immuno electrode is let to dry for overnight. After which 25 µl of 1mgmL^{-1} BSA is poured onto the immuno-electrode, which facilitates the blocking of active sites. Now, this BSA/APTES/Fe-MoO_3/ITO electrode is kept at room temperature for 3- 4 hrs for drying. After this the immuno-electroe is washed with PBS buffer, which removes the unbound antibodies. After the immuno-electrode is dried, is analysed.

Figure 3.11: Immobilization (Drop casting) and washing of immuno-electrode

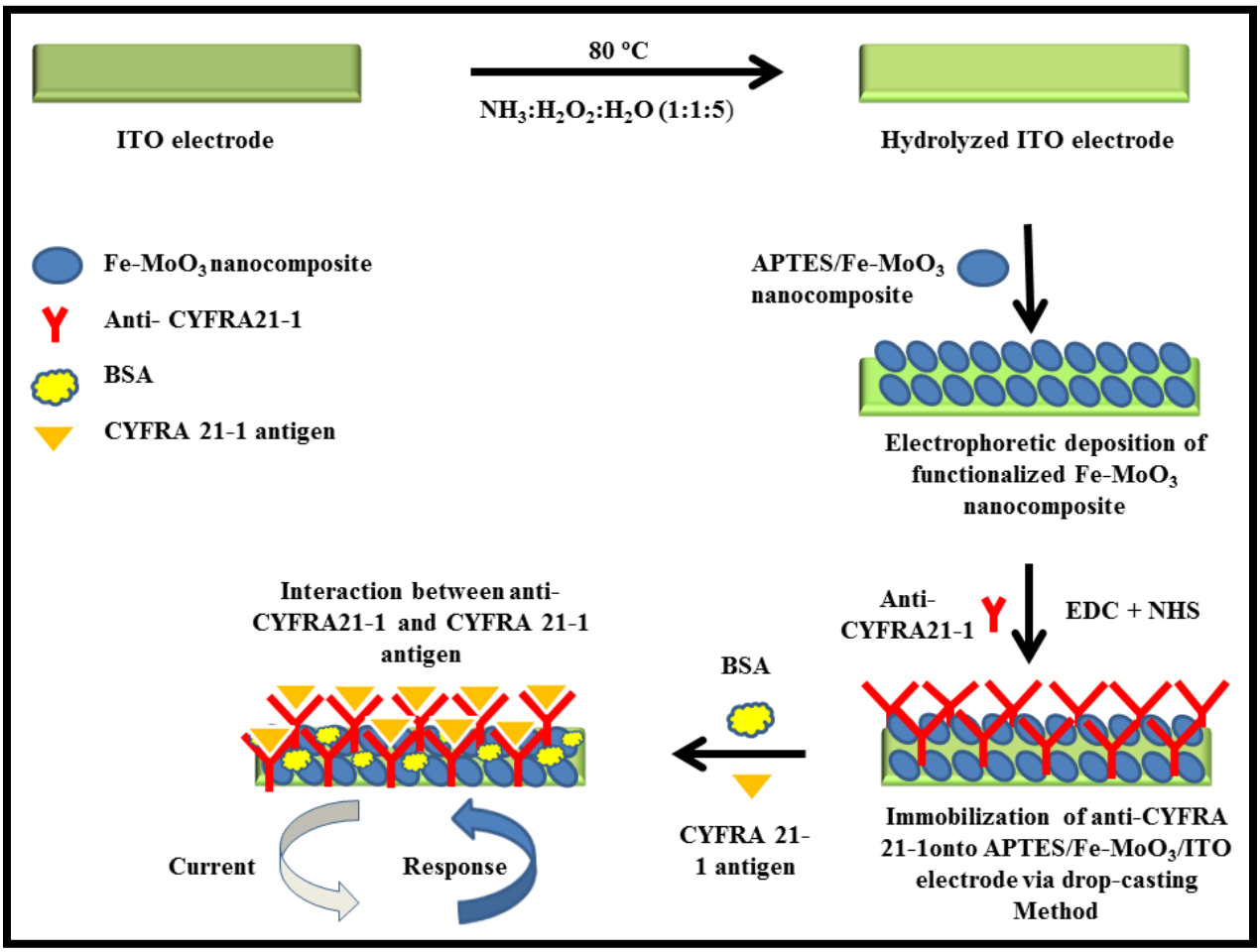

Figure 3.12: Schematic showing the fabrication of bio sensing platform

CHAPTER-4

RESULTS AND DISCUSSION

Structural and morphological studies of MoO_3/Fe-MoO_3

4.1) X- Ray Diffraction :

XRD studies were conducted to investigate the crystallinity and phase of the synthesized MoO_3 and Fe- MoO3. For MoO_3 major peaks were observed at 12.7º, 23.30º, 25.64º, 27.28º, 38.94º, 58.77º corresponding to the plane?????. The peak with the maximum intensity was observed at 25.64º corresponds to the plane (040), having orthorhombic lattice system with lattice parameters a= 3.962 Aº, b=13.85 Aº and c=3.701Aº (JCPDS 895108). Likewise, for Fe-MoO3, the intensity o fthe peaks were found to be reduced due to incorporation of Fe the high crystalline peaks of MoO_3 resultant in broader peaks. The maximum intensity peak obatine in the composite was at 27.82º correspond to the plane (201), having a monoclinic lattice system with lattice parameters a= 9.805 Aº, b= 8.950 Aº and c= 7.660 Aº (JCPDS 892366). Peak with the maximum intensity was observed Since the size of the synthesized nanoparticle plays a very important role in determining the efficiency of the biosensor. *(Kumar et al, 2016)*

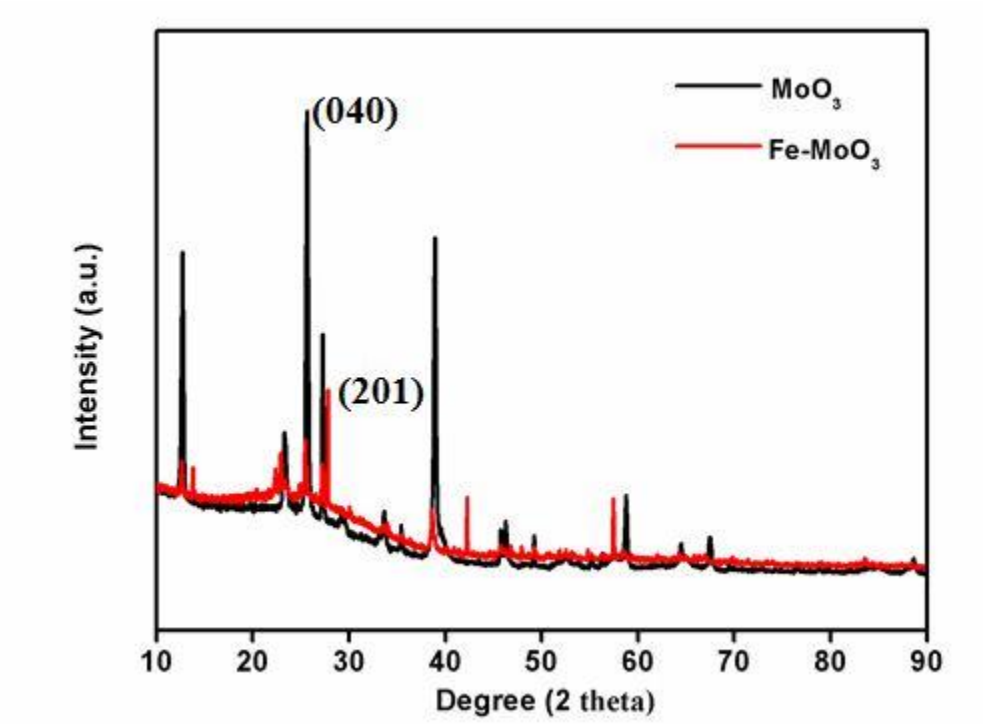

Figure 4.1: XRD graph of MoO_3 and Fe-MoO_3 obtained from Bruker D-8, U.S.A

By using Debye-Schrrer equation, using the maximum intensity peak of synthesized MoO_3 nanostructure, the size of MoO_3 nanostructure were calculated. Debye-Scherrer formula:

Size of (D) = Kλ/ β Cosθ

Where:

K = shape factor

λ = X-Ray wavelength (nm)

β = Full width half maxima

θ = Braggs angle (radian).

The size of synthesized Fe-MoO_3 nanostructure was 22.7 nm ~ **23 nm**.

4.2) <u>Scanning electron microscope (SEM)</u>

SEM studies were carried out to investigate the morphology of MoO_3 and Fe- MoO_3, SEM was carried out. The SEM images of MoO_3, which is shown in the figure, indicates a rod like structure, confirming the formation of MoO_3 nanorods as shown in the figure (a) Figure (b) shows the SEM image of Fe-MoO_3 nanocomposite, showing the dispersed nano rods of MoO_3 into the clusters of Fe, with decreased width of nano rods from initial and also with a spindle pointed shape, onto which the Fe nanoparticles have been attached.

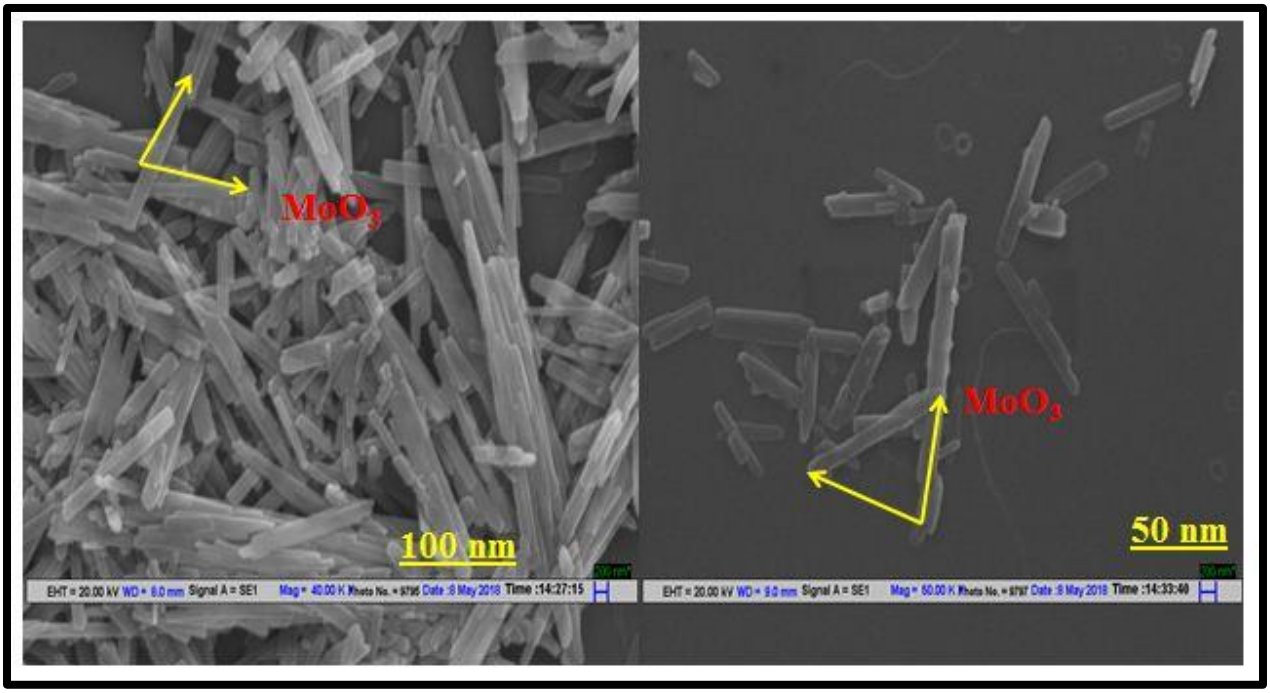

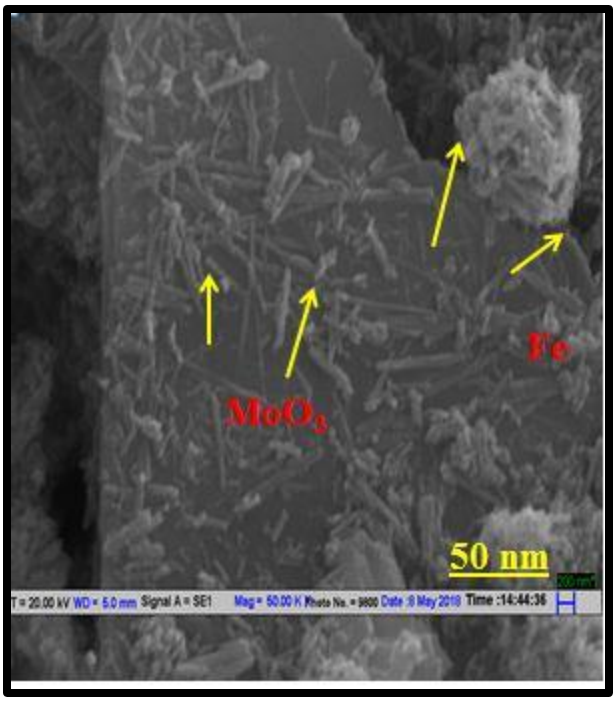

Figure 4.2: Scanning electron microscope image of MoO_3 and Fe-MoO_3 taken from Hitachi S-3700N, Japan

4.3) FT-IR Spectroscopy:

FT-IR studies were conducted for MoO_3, Fe-MoO_3, and APTES/Fe-MoO_3 respectively to investigate the functional group. Spectra of the synthesized MoO_3, Fe-MoO_3, APTES/Fe-MoO_3 were observed in the range of 500-4000 cm^{-1} . In case of MoO_3 a broad peak at 3472 cm and 1638 cm appeared, which is due to stretching and bending vibration of hydroxyl groups absorbed on molybdenum oxide nanoparticle. The peak at 999 cm^{-1} is due to the terminal M=O bond which indicate the layered orthorhombic phase and the peak at 866 cm^{-1} shows the stretching mode of vibration M-O-M *(Dighore et al, 2014).* In Fe-MoO_3 and APTES/Fe-MoO_3,the peaks at 1706 and 1426 cm^{-1} were observed which, shows the presence of Fe-Mo bonds in the samples. An additional peak at 3483 cm^{-1}, in APTES/Fe-MoO_3 sample were observed, which is due to the presence of primary amide (-NH_2) bond.

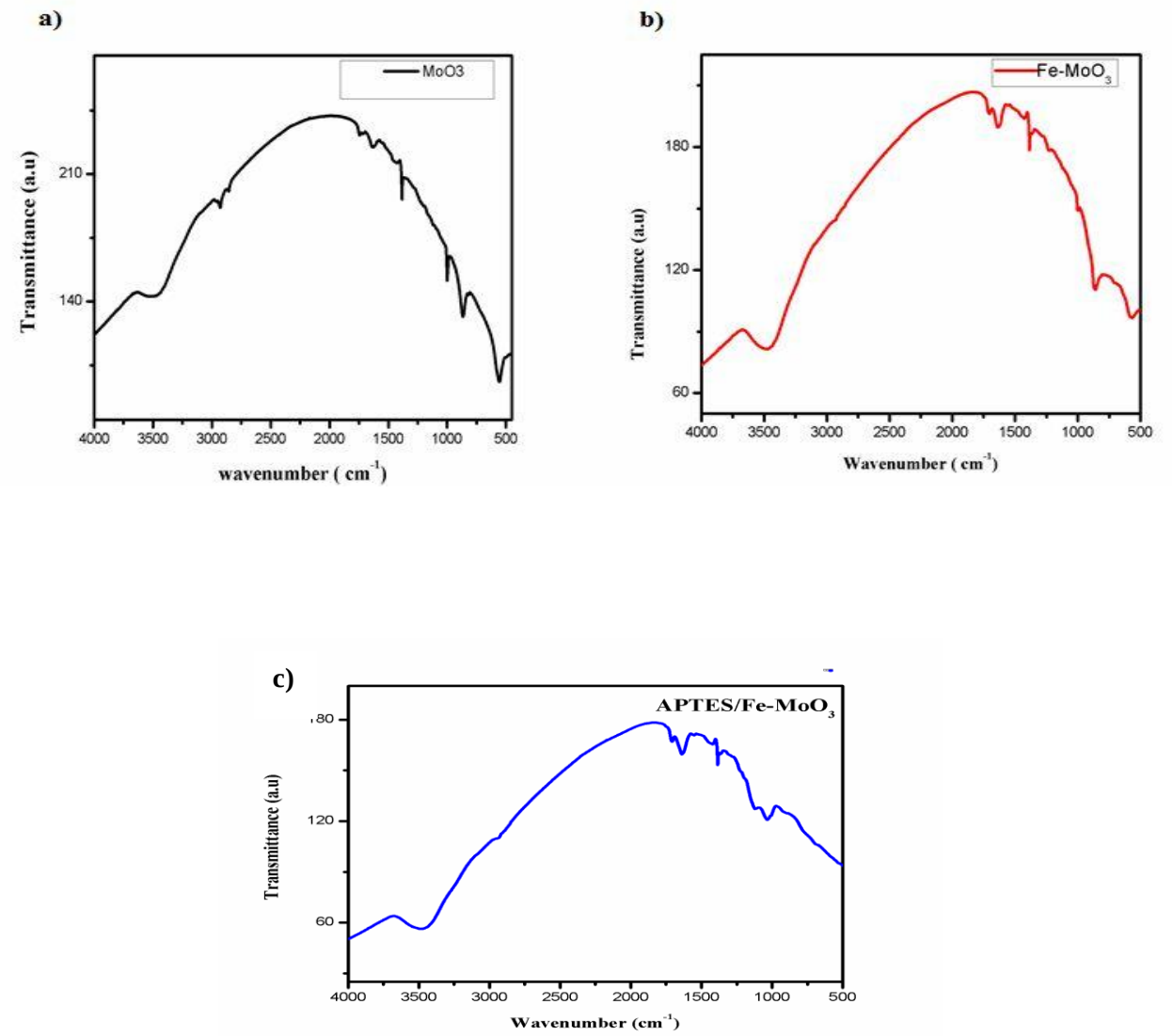

Figure 4.3: FT-IR spectra of (a) MoO_3, (b) Fe-MoO_3, (c) APTES/Fe-MoO_3

4.4) UV- Spectrophotometry:

The UV studies of MoO_3 and nanocomposite of Fe-MoO_3 were performed in a wavelength range of 200-400 nm, which gives the general idea about the formation of MoO_3 nanoparticles and Fe-MoO_3 nano-composites. A peak at 213 nm was observed, which confirms the presence of MoO_3 nanoparticle. Additional peak at 235 nm was observed, which shows the presence of Fe in MoO_3.

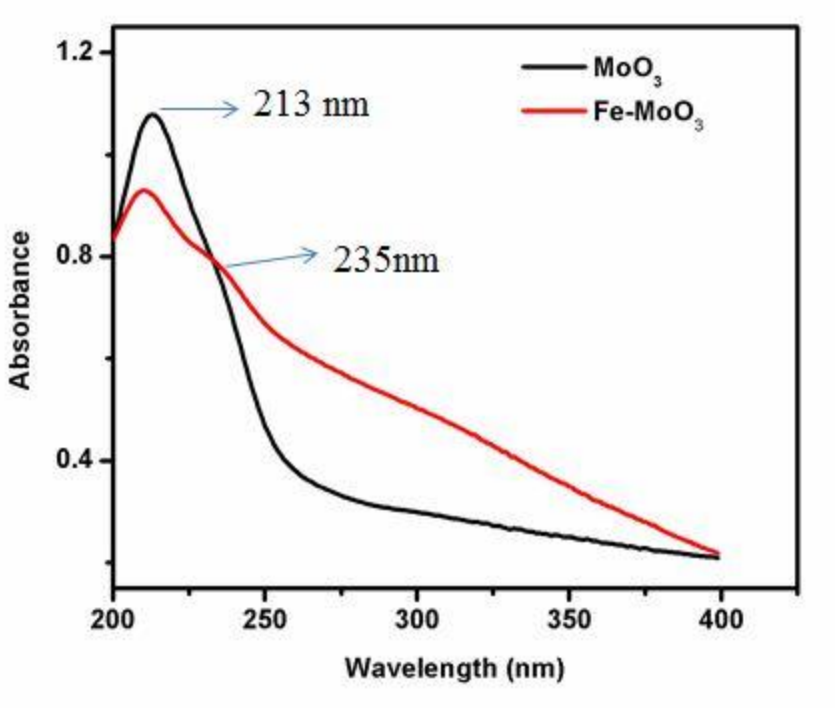

Figure 4.4: UV Spectra of MoO_3 and Fe-MoO_3

4.5) Dynamic light scattering (DLS) :

DLS studies were conducted for the synthesized MoO_3 and Fe- MoO_3 nanocomposite, which shows the hydrodynamic radius of synthesized nanoparticle and nanocomposite respectively. For this, the synthesiszed MoO_3 and Fe-MoO_3 were dissolved in D.I and EthanolFrom the DLS study (Figure ??????????), an idea for the size of synthesized nanoparticle can be estimated. The size observed from the DLS study was found to be in the range > 100 nm in both the casaes This may be due to the reason that aggregation of the nanocomposite results in the increased size of the nanomaterial . Moreover the DLS study analyses the nanomaterial into a spherical form then calculates the size . In this case the nanorods are assumed as the spherical structure resulting in increased size.

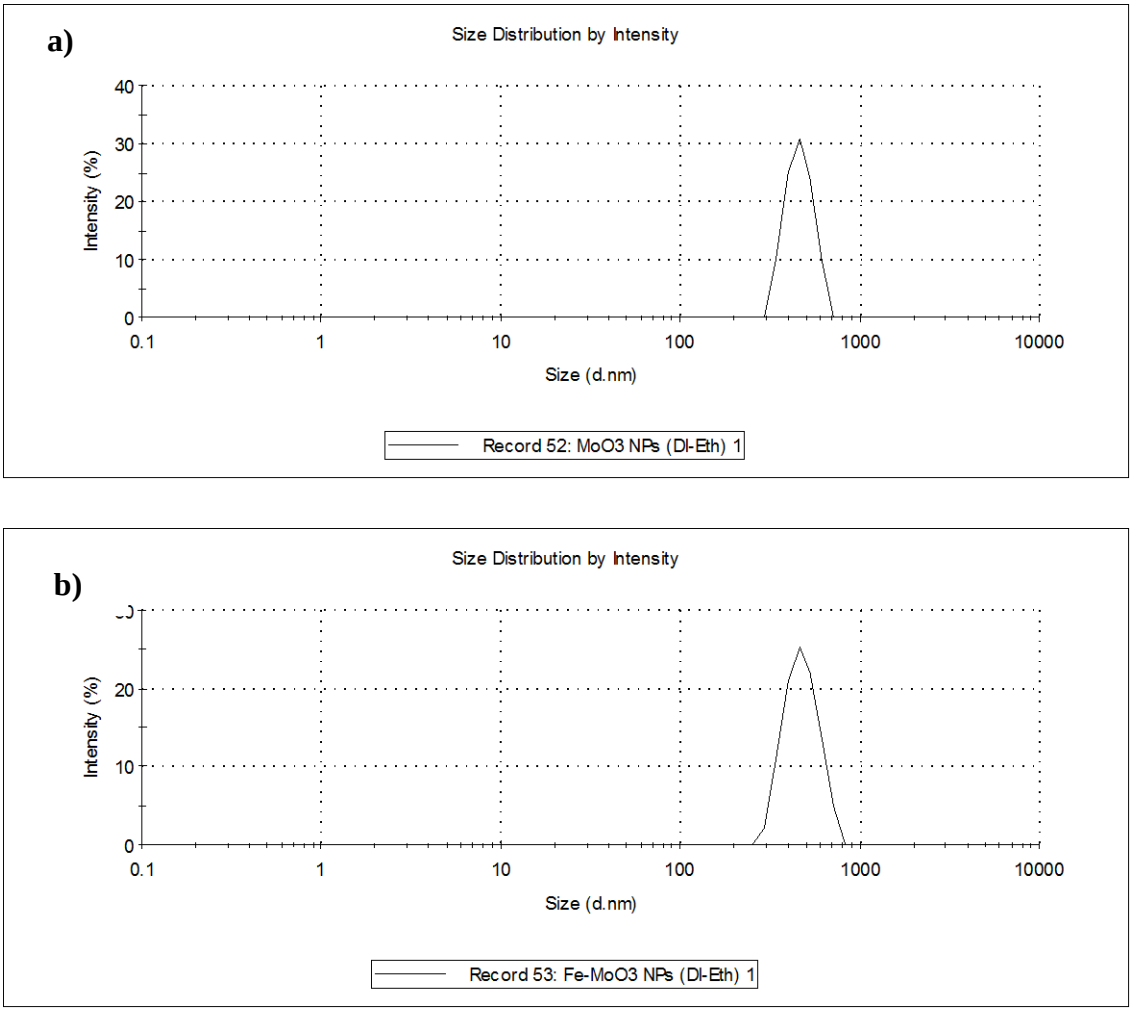

Figure 4.5: Dynamic light scattering (DLS) graph of (a) MoO_3 and (b) Fe- MoO_3

4.6) Electrochemical studies:

4.6.1) Fe-Optimization in Fe-MoO_3

For the synthesized Fe-MoO3 nanocomposite, the content of Fe were optimized, Different weight ratio of ferrous sulphate ($FeSO4.7H_2O$) to precursor salt, sodium molybdate (NaMoO4.2H2O) (i.e. 0.5%, 2%, 5%,) were taken, and were synthesized by hydrothermal method, and electrode (Fe-MoO_3/ITO) were fabricated. The electrochemical studies of the different electrode of MoO_3/ITO, Fe –MoO_3/ITO were carried out via DPV technique (shown in figure ……) using PBS solution (50 mM, pH 7.0, 0.9% NaCl) containing 5 mM of [Fe(CN)6]3-/4- at a scan rate of 10 mV s-1 in the potential range, -0.6 to 0.6V. It was observed that the magnitude of peak current obtained for MoO3/ITO electrode is 0.20 mA. Whereas the electrochemical response for the fabricated electrodes with different Fe content exhibited current as with 0.5% was 0.19 mA, which was lower than the reference value of 0.20 mA . Similarly, for 2% , the value of peak current observed was 0.26 mA, and for 5%, the value of peak current was found to be 0.35 mA , which was maximum amongst all. Hence the Fe content in Fe-MoO3 nanocomposite were optimized to 5%. The increase in the current behavior in the nanocomposite is attributed to the replacement of Mo by Fe, causing lattice distortion, due to which increased in the surface area, and more exposure to the active sites for reaction and hence electrochemical activity of nanocomposite gets increased resulting in higher value of current. (.(Ruiliang et al., 2013).)

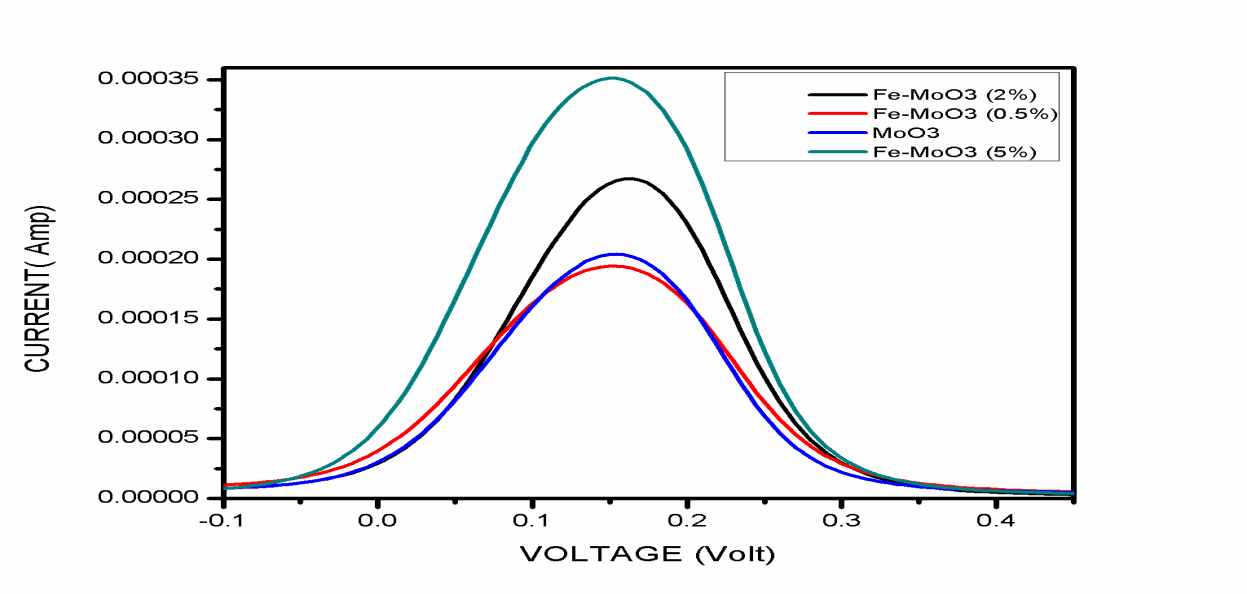

Figure 4.6: Differential pulse voltammetry (DPV) of MoO_3/ITO, Fe-MoO3/ITO(0.5%), Fe-MoO_3/ITO (2%), Fe-MoO_3/ITO (5%)

*4.6.2) **Electrode studies:***

The DPV studies on MoO_3/ITO, Fe-MoO_3/ITO, APTES/Fe-MoO_3/ITO, and anti-CYFA-21-1/APTES/Fe-MoO3/ITO electrodes respectively in PBS solutions (50 mM, pH 7.0, 0.9% NaCl) containing 5 mM of [Fe(CN)6]3-/4- at a scan rate of 10 mV s-1 in the potential range, -0.6 to 0.6V. It was found that the magnitude of peak current obtained for MoO_3/ITO electrode is 0.26 mA and in case of the Fe-MoO3/ITO electrode is 0.41mA. this is attributed due to the nanocomposite, due to the replacement of Fe from Mo, causing lattice distortion, due to which increased in the surface area, and more exposure to the active sites for reaction and hence electrochemical activity of nanocomposite gets increased resulting in higher value of current.(*Ruiliang et al., 2013*). After immobilization of the antibodies i.e. anti-CYFRA-21-1/APTES/ Fe-MoO_3/ITO immuno-electrode shows decrease in peak current i.e. 0.32 mA, which may be due to the binding of the antibody. Since antibodies are the biomolecules having insulating nature, due to which the electrical conductivity slows down as it gets bind to the nanomaterial.

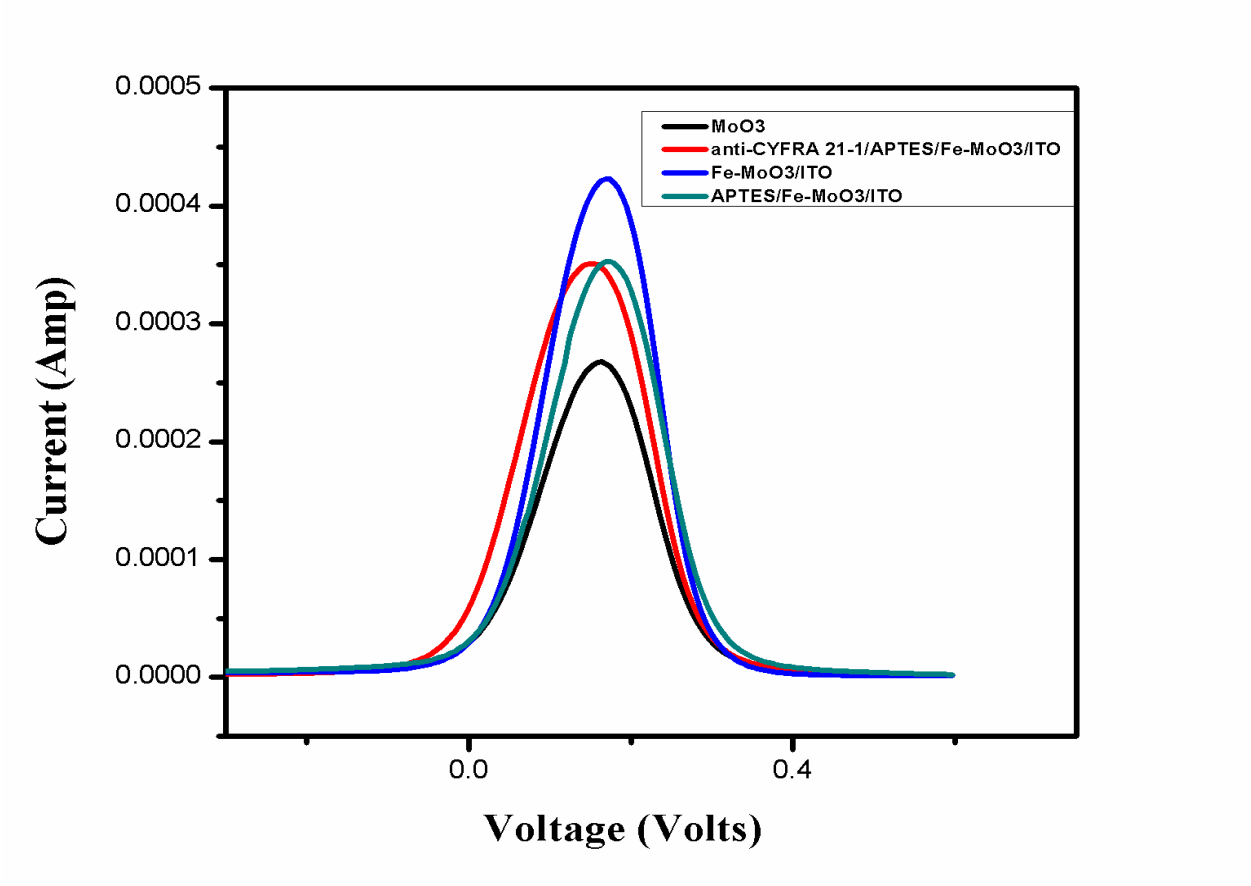

Figure 4.7: Differential pulse voltammetry (DPV) of MoO_3/ITO, Fe-MoO_3/ITO, APTES/Fe-MoO_3/ITO, anti- CYFRA21-1/APTES/Fe-MoO_3/ITO

4.6.3) pH studies

pH studies of the BSA/anti-CYFRA-21-1/APTES/Fe-MoO3/ITO immunoelectrode were carried out using differential pulse voltammetry (DPV) technique, as a function of pH (6 to 8) at the scan rate of 10 mV s^{-1} in PBS containing 5×10^{-3} M $[Fe(CN)_6]^{3-/4-}$. It can be seen that the maximum peak current was obtained at neutral pH 7. This is due to the fact that biological molecules such as amino acids, antigen, antibody, enzymes etc. are present in natural form at with high specific activity at neutral pH. Therefore, in acidic or basic medium antibodies get denatured due to the interaction H+ or OH- ion on amino acid sequence of antibodies. Thus, PBS buffer with pH 7 was used for all the electrochemical studies.

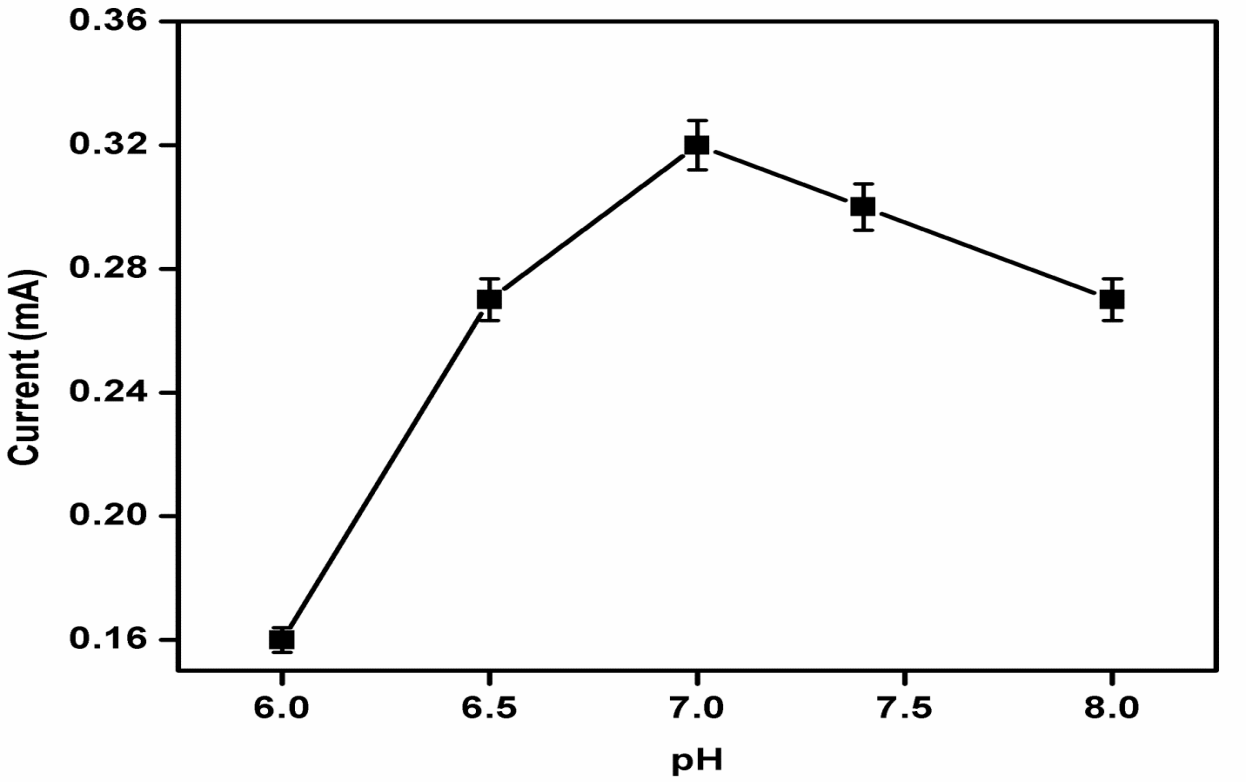

Figure 4.8: Current response of BSA/anti-CYFRA21-1/APTES/Fe-MoO_3/ITO immuno-electrode at different pH values

4.6.4) <u>Scan rate studies</u>:

i) <u>Without CYFRA21-1 (APTES/Fe-MoO_3/ITO)</u>

The cyclic voltammetry (CV) response of APTES/Fe-MoO3/ITO and BSA/anti-CYFRA-21-1/APTES/Fe-MoO3/ITO electrodes was shown as a function of scan rate (40-140 mV s-1), respectively. We observed that the magnitude of both cathodic (Ipc) and anodic (Ipa) peak current exhibit a linear relationship with the square root of scan rate, indicating the electrochemical reaction is a diffusion-controlled process.

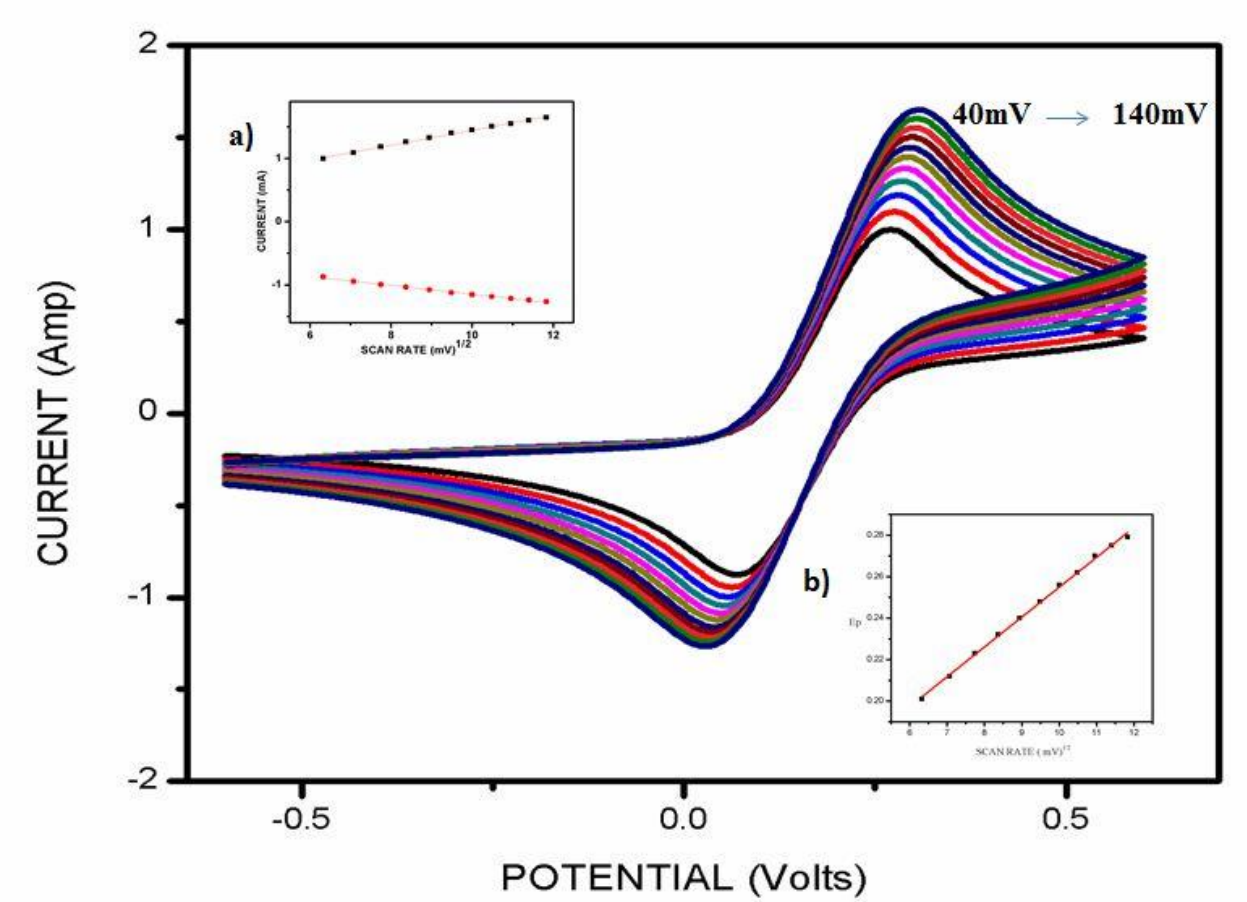

Figure 4.9: <u>Cyclic voltammetry (CV) of anti-CYFRA21-1/APTES/Fe-MoO_3/ITO electrode as a function of scan rate (40-190 mV/s). Magnitude of oxidation and reduction current response as a function of scan rate (mV/s) (inset a), and difference of cathodic and anodic peak potential (ΔEp) as a function of scan rate (inset b).</u>

ii) With CYFRA21-1(BSA/anti-CYFRA21-1/Fe-MoO_3/ITO)

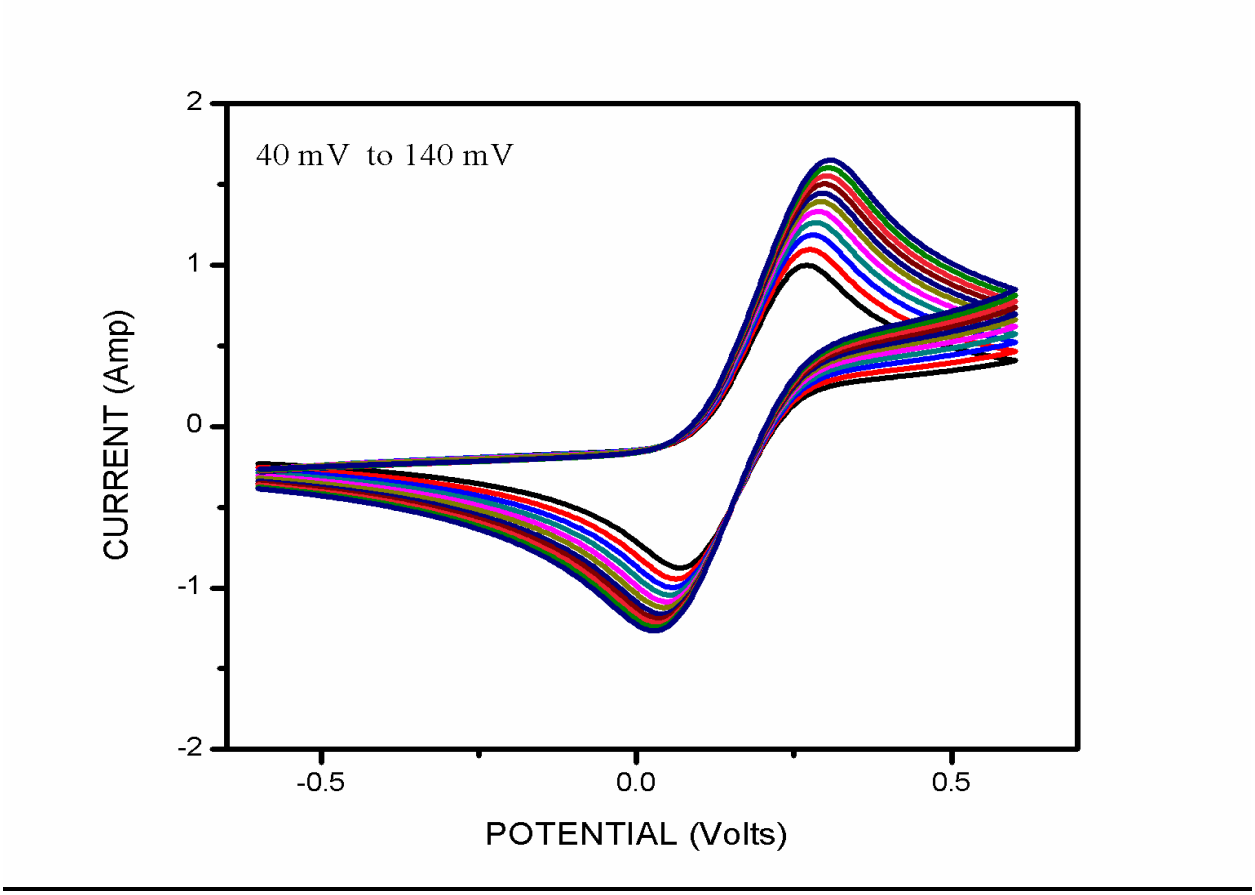

4.6.5) Electrochemical response studies:

The electrochemical studies of the fabricated immuno- electrode (BSA/anti-CYFRA21-1/APTES/Fe-MoO_3/ITO) were conducted by Differential Pulse Voltammetry (DPV) technique against CYFRA-21-1 concentration in PBS buffer (50 mM, 0.9% NaCl) containing [Fe(CN)6]3-/4- (5 mM) using a three electrode system . The fabricated immunoelectrode was taken as the working electrode, platinum as counter electrode, and Ag/AgCl as the reference electrode After which the immuno-electrode was left for 40 mins incubation. Different concentration of CYFRA-21-1 were added from 2ng/ml to 32 ng/ml, and corresponding to which three DPV readings for each concentration were recorded. It has been found that with increasing g concentration of CYFRA-21-1 the magnitude of anodic peak current decreased. This decrease

may be attributed to the to the formation of antigen-antibody complex between CYFRA-21-1 and anti-CYFRA-21-1 on the electrode. *(Kumar et.al, 2013)*

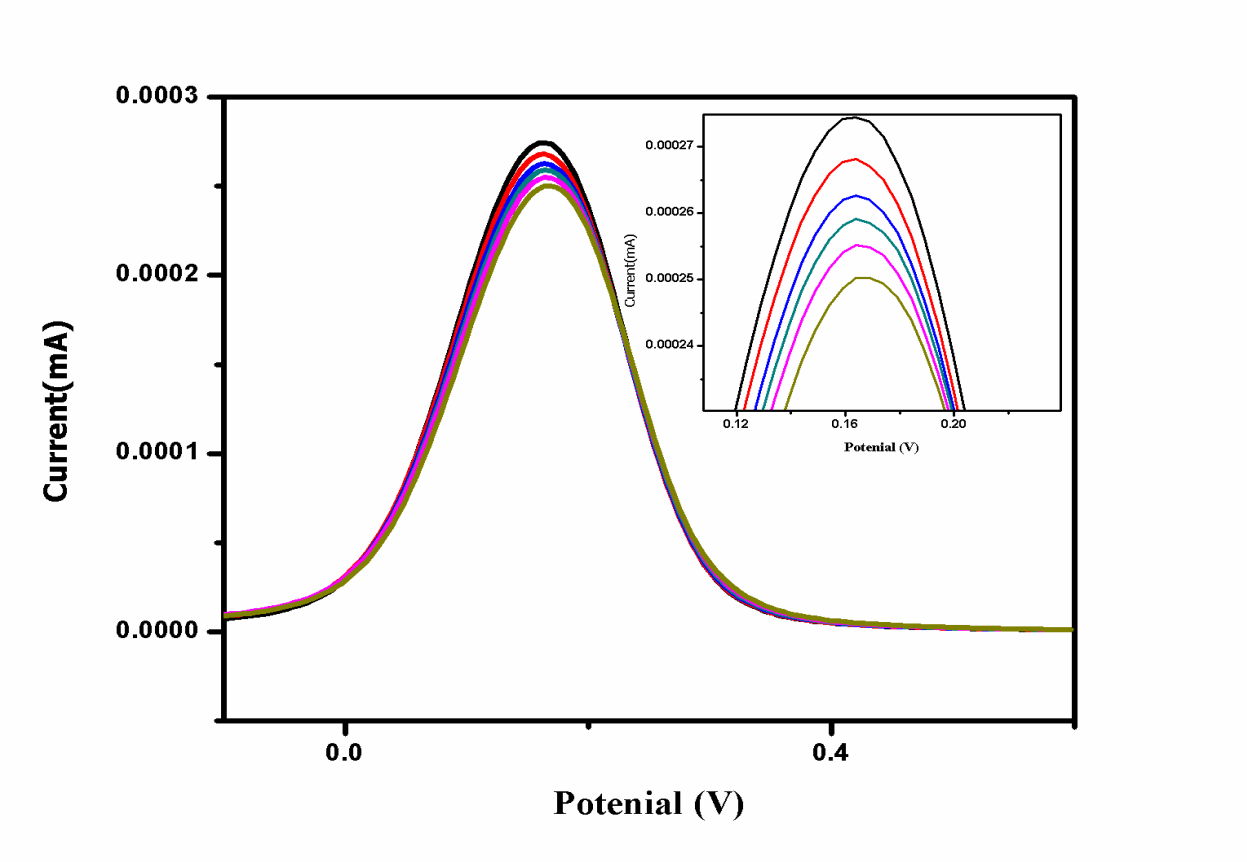

Figure 4.11: Electrochemical response of BSA/anti-CYFRA-21-1/APTES/Fe-MoO_3/ITO immunoelectrode as a function of CYFRA-21-1 concentration (2.0-32 ng mL-1).

Under the above optimized conditions, the curve between different concentration of CYFRA-21-1 and BSA/anti-CYFRA-21-1/APTES/Fe-MoO_3/ITO immuno-electrode was plotted which, shows linear range in the concentration of 2.0 to 32 ng mL-1. After which the current tends to saturate at higher concentrations with a linear regression coefficient of 0.98907. The sensitivity of the fabricated immune-oelectrode can be estimated by the slope of the curve and is found to be 0.01462 mA ng-1 mL. The limit of detection and standard deviation of the immuno-electrode

are obtained to be 0.157 ng/ml and 76.5 ng mL-1. The limit of detection has been calculated using the standard equation:

Limit of detection (LOD) = 3σ/sensitivity

After which the current tends to saturate at higher concentrations can be estimated by the slope of the curve and is found to be ^{2}. The limit of detection and standard deviation of the immunoelectrode are obtained to be 0.157 ng/ml and 76.5 ng mL-1. The limit of detection has been calculated using the standard equation:

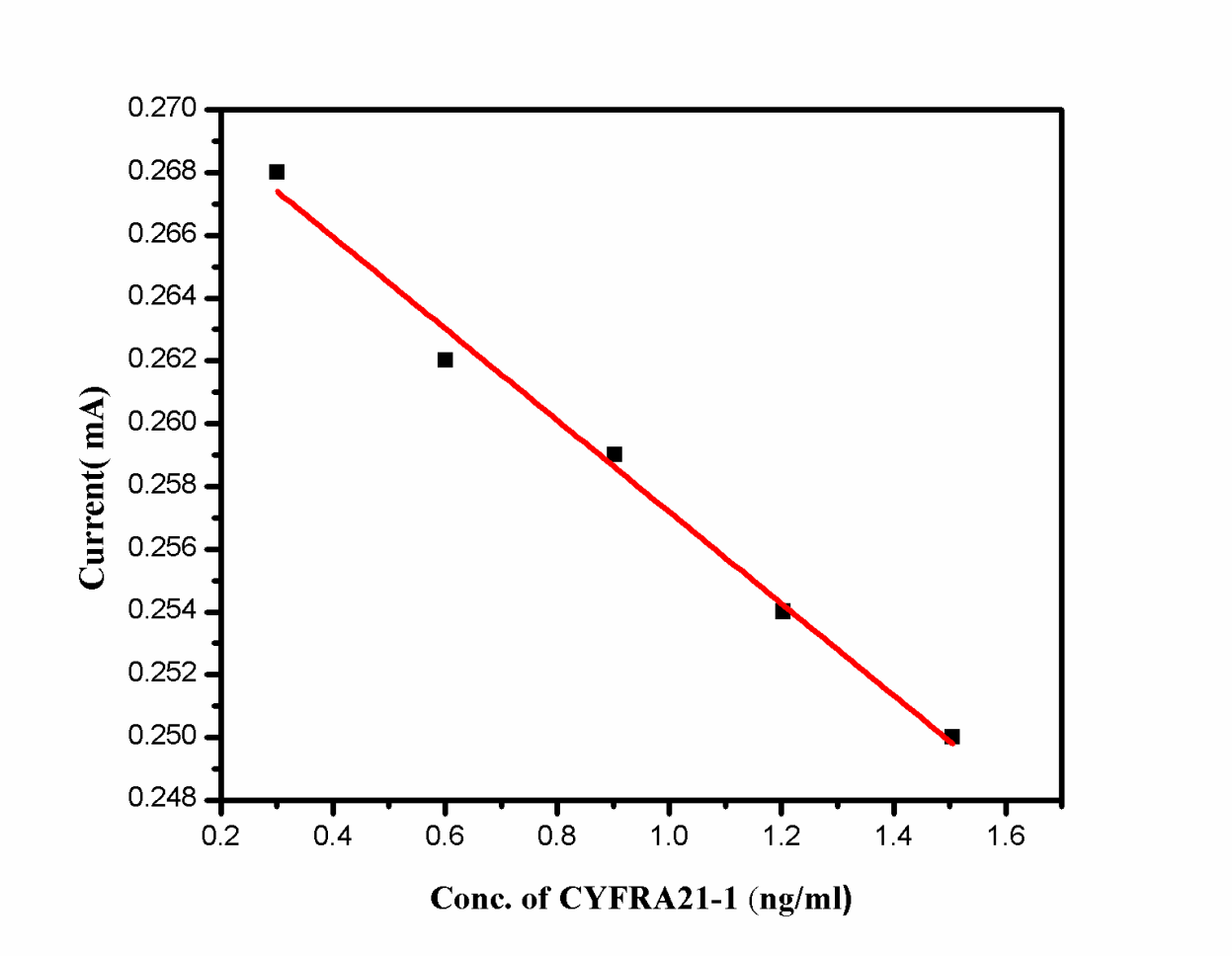

Figure 4.12: Calibration curve between magnitude of peak current and concentration of CYFRA-21-1 (ng mL-1)

CHAPTER-5

CONCLUSION

Conclusion

We have proposed a biocompatible Fe-MoO3 nanocomposite, based point of care device, which is an efficient, label free and robust bio sensing platform for breast cancer biomarker (CYFRA-21-1) detection using blood serum. First of all, we have synthesized a nanocomposite of Fe-MoO3 by hydrothermal method, further in which Fe content was optimized to 5%, starting from 0.5%, 1%, 2% and 5%. After which, the Fe-MoO_3 nanocomposite was functionalized with APTES by simple chemical process. The functionalized, nanocomposite was Electrophoretically deposited on pre hydrolyzed ITO glass electrode. Further the obtained thin film of APTES/Fe-MoO_3/ITO was bio functionalized with anti-CYFRA-21-1 with the help of EDC-NHS covalent surface chemistry and BSA was used to block the non-specific binding sites of immuno-electrode. The fabricated BSA/anti-CYFRA-21-1/APTES/Fe-MoO_3/ITO is simple and covers the whole physiological range of CYFRA-21-1, present in human blood serum samples i.e. 2 ng/ml to 32 ng/ml, with linear detection range ng mL-1, sensitivity 0.01462 mA mg-1 mL ng-1. Limit oof detection for the above fabricated biosensor was 0.157ng/ml. Fabrication of nanocomposite of Fe-MoO_3, opens a new scope in fabrication of bio sensing platform as well as in drug delivery, tissue repair and in bio imaging systems, by exploiting its magnetic properties.

CHAPTER-6

FUTURE PERSPECTS

Future perspects

The present experimental investigations reveal that the nanocomposite of MoO_3 with Fe can efficiently be utilized in the development of high performance electrochemical bio sensing or point of care devices with high sensitivity, selectivity, stability and design flexibility for both laboratory and point-of-care applications. Further, this nanocomposite could be utilized in the detection analysis and quantification of various other biomarkers expressed in different diseases i.e. oral cancer, colon cancer etc. Besides this, studies should be carried out to explore the application of these matrices for the development of toxin biosensors and other immuno-sensors. Also the properties of synthesized nanocomposite could be used, with combinations of different biomarkers in order to diagnose and detect the disease condition,

Recently, microfluidics technology coupled with Nano science and nanotechnology are becoming powerful tools in biosensors fabrication, due to the advantages of high performance, design flexibility, reagent economy, high throughput, miniaturization, and automation. These miniaturized chip devices can notably change the speed and scale towards highly specific and selective antibody–antigen interactions. Attributing to the interesting physiochemical properties of the Fe-MoO_3, it would be interesting to incorporate Fe-MoO_3 and there derivative in microfluidic devices. Also the above synthesized nanocomposite has a magnetic property which could also be exploit for target drug delivery and cell imaging, apart from this it could also be used in various bio separation processes and in down streaming. This further opens a new area of research and probably meet the real challenge in high performance bio sensing and biomedical applications.

CHAPTER-8

REFERENCES

References

- Chapman, M, et al. “Circulating CYFRA 21-1 is a Specific Diagnostic and Prognostic Biomarkerin Biliary Tract Cancer” *Journal of clinical and experimental hepatology.* (2011).
- Gao, Arnan, et al. “ Robust Ultrasensitive tunneling FET biosensor for point of care devices” *Scientific Reports Nature* (2016).
- Gunda, Nagashiv et al. “ Optimization and characterization of biomolecule immobilization on silicon substrates using APTES and gluteraldehyde linkers” *Applied Surface Science* 305(2014): 522-530.
- Kumar, Saurabh, et al. "Reduced graphene oxide modified smart conducting paper for cancer biosensor." *Biosensors and Bioelectronics* 73 (2015): 114-122.)
- Kumar, Suveen, et al. "Nanostructured zirconia decorated reduced graphene oxide based efficient biosensing platform for non-invasive oral cancer detection." *Biosensors and Bioelectronics* 78 (2016): 497-504.).
- Kumar, Suveen et al. “ Effect of browian motion on reduced agglomeration of nanostructured metal oxide towards development of efficient cancer biosensor ” . *Biosensors and bioelectronics* 102 (2018): 247-255).
- Kumar, V, et al. “ Localized charge transfer in two-dimensional molybdenum trioxide” *Applied materials and interfaces.* 9(2017) 045-053.
- Marakkchi, R, et al. “ Detection of Cytokeratin 19 m RNA and CYFRA 21-1 in blood of tunisian women with breast cancer”. *The International Journal of Biological markers* 23 (2008): 238-243).
- Mikkelsen,G, et al.” Reference limit of chromogranin A, CYFRA21-1,CA-125, CA19-9,and carcinoembryonic antigen in patients with chronic kidney disease”. *International Journal of Biological markers.*(2017).
- Murphy, Katrina. “ The effect of annealing metallic nanoparticles on their catalytic efficiency” *Material NNIN REU Research accomplishment* (2006).
- Nakata, Bunzo, et al. “ Serum CYFRA21-1 is one of the most reliable tumor markers for breast carcinoma”. *American Cancer Society* 89(2000).
- Rajkumar,K,et al.” Salivary and serum level of CYFRA 21-1 in oral precancer and oral squamous cell carcinoma” *Oral disease.* 21(2015)90-96.
- Tartaj, Pedro, et al. “ The preparation of magnetic nanoparticles for application in biomedicine”. *Journal of Applied Physics* 36(2004): 182-197.
- Wang, Longquik et al. “ Synthesis of crystalline/amorphous core /shell MoO_3 composites through a controlled dehydration route and their enhanced ethanol sensing properties” *American Chemical Society* 14 (2014): 569-575.
- Wang, H, et al. “Flower-like Fe2O3@MoS2 nanocomposite decorated glassy carbonelectrode for the determination of nitrite” *Sensors and Actuators B* 220(2015):749-754.

- Xu, R, et al. " One-step synthesis and the enhanced xylene-sensing properties of Fe-doped MoO3 nanobelts" *Royal Society of Chemistry* 00(2013): 1-3.
- Thévenot et al, "Electrochemical biosensors: recommended definitions and classification", *Biosensors and Bioelectronics*, 16(2001) 121-31.
- Koyun A, et al, "Biosensors and their principles", *A Roadmap of Biomedical Engineers and Milestones*, (2012).
- Gerard M et al, " Application of conducting polymers to biosensors", *Biosensors and Bioelectronics*, 17(2002) 345-59.
- Ahuja T et al, "Biomolecular immobilization on conducting polymers for biosensing applications ", *Biomaterials*, 28(2007) 791-805.
- Ansari A.A et al, " Nanostructured metal oxides based enzymatic electrochemical biosensors": *INTECH Open Access Publisher*; 2010.
- Ansari A. A et al, " Recent advances in nanostructured metal oxides based electrochemical biosensors for clinical diagnostics", *Nova Science Publishers: Hauppauge, NY, USA* 2009.
- Sinclair I, "Sensors and transducers", *Newnes*; 2000.
- Solanki P.R et al , "Nanostructured zirconium oxide based genosensor for Escherichia coli detection ", *Electrochemistry Communications*, 11(2009) 2272-7.
- Macaluso M et al, " Genetic and epigenetic alterations as hallmarks of the intricate road to cancer", *Oncogene*, 22(2003) 6472-8.
- Clapp R.W et al, " Environmental and occupational causes of cancer: a call to act on what we know", *Biomedicine & Pharmacotherapy*, 61(2007) 631-9.
- Thun M.J et al, "The global burden of cancer: priorities for prevention", *Carcinogenesis*, 31(2010) 100-10.